

# We are IntechOpen, the world's leading publisher of Open Access books Built by scientists, for scientists

4,800

Open access books available

122,000

International authors and editors

135M

Downloads

Our authors are among the

154

Countries delivered to

TOP 1%

most cited scientists

12.2%

Contributors from top 500 universities



WEB OF SCIENCE™

Selection of our books indexed in the Book Citation Index  
in Web of Science™ Core Collection (BKCI)

Interested in publishing with us?  
Contact [book.department@intechopen.com](mailto:book.department@intechopen.com)

Numbers displayed above are based on latest data collected.  
For more information visit [www.intechopen.com](http://www.intechopen.com)



# Open-Path FTIR Detection of Explosives on Metallic Surfaces

John R. Castro-Suarez<sup>1</sup>, Leonardo C. Pacheco-Londoño<sup>1</sup>,  
Miguel Vélez-Reyes<sup>2</sup>, Max Diem<sup>3</sup> and Thomas J. Tague, Jr.<sup>4</sup>  
and Samuel P. Hernandez-Rivera<sup>1</sup>

*ALERT DHS Center of Excellence for Explosives  
Center for Chemical Sensors Development*

<sup>1</sup>*Department of Chemistry, University of Puerto Rico, Mayagüez, PR*

<sup>2</sup>*Department of Electrical Engineering, University of Puerto Rico, Mayagüez, PR*

<sup>3</sup>*Department of Chemistry, Northeastern University, Boston, MA*

<sup>4</sup>*Bruker Optics, Billerica, MA 01821*

<sup>1,2</sup>*Puerto Rico*

<sup>3,4</sup>*U.S.A*

## 1. Introduction

Defense and security agencies are in constant demand of new ways of detecting chemical and biological threats posed by terrorist organizations. Fundamental and applied research in areas of interest to national defense and security focus in detection of highly energetic materials (HEM), including homemade explosives (HME) that could be used as weapons of mass destruction (Marshall and Oxley, 2009; Yinon and Zitrin, 1996; Schubert and Rimski-Korsakov, 2006). The Department of Homeland Security of the United States of America has even gone a step further and established a university based Center of Excellence in explosives detection, mitigation and response to conduct transformational research, technology and educational development for effective characterization, detection, mitigation and response to the explosives-related threats facing the country and the world. The Awareness and Localization of Explosives Threats (AWARE) is co-lead by Northeastern University (ALERT at NU, Boston, MA) and University of Rhode Island (ALERT at URI, Kingston, RI).

Current detection methods of explosives are based on a wide variety of technologies that focus on either bulk explosives or traces of explosives. Bulk explosives can be detected indirectly by imaging characteristic shapes of the explosive charge, detonators, and wires or directly by detecting the chemical composition or dielectric properties of the explosive material. Trace detection methods rely on detection of vapors emitted from the explosives or on explosive particles that are deposited on nearby surfaces (National Academy of Sciences Committee, 2004). Although there are hundreds of publications about methods of detection of HEM in water, soil, air, clothing, surfaces, etc. and these offer the advantage of providing very low limits of detection at ppb levels (Caron, et al., 2010; Hilmi and Luong, 2000; Yinon, 1996; Szakal and Brewer, 2009; Miller and Yoder, 2010). They require, in the majority of the cases, sampling at the scene followed by a sample preparation step, to be later analyzed by a

particular technique. Sampling and sample preparation are among the main disadvantages in HEM detection, in many cases threatening the health and life of analysts and first responders. Vibrational spectroscopy, in its various modalities, has shown to be useful for detection of dangerous chemicals, among them HEM. Near-infrared or mid-infrared spectroscopies have shown to be powerful techniques for IR vibrational analysis, able to detect organic and inorganic substances in any state: solid, liquid or gas (Gunzler, 2002; Smith, 2000). IR vibrational spectra can be used to identify and quantify samples in complex matrices because each substance has its own fingerprint spectrum in the mid IR (MIR). This means that IR spectroscopy can be used for discriminant analysis even when the target analyte is in very small quantities (Bangalore, 1997).

Standoff detection is defined as where equipment and operator stay away from the sample while measuring some property of the target (Parmenter, 2004). An area of IR spectroscopy that has increased interest in defense and security applications is standoff IR (SOIR) spectroscopy. In SOIR detection, vibrational signatures can be recorded from several meters to hundreds of meters in distances between the target and the instrument. Fourier transform infrared (FTIR) standoff detection provides a means of doing real time analysis, in which no sample preparation is needed, no human contact needs to be provided, measurements are typically fast, and chemical information for each explosive can be obtained in high detail which can allow identification and even quantification. This makes the standoff IR detection a powerful technique for sensing of energetic materials at a distance, thus preventing or minimizing the damage caused by terrorist action, in the case that this comes to be detonated.

Open-Path Fourier Transform IR (OP/FTIR) spectroscopy has been used for atmospheric gas analysis and environmental monitoring for over 40 years (Griffiths, et al., 2009). It is one of the two methodologies devised for measuring concentration of gaseous trace components in the atmosphere using infrared spectroscopy: extractive sampling analysis and *in situ* open-path analysis. Although Russwurm and Childers credit Hanst for the initial description of FTIR monitoring of atmospheric pollutants in the atmosphere by OP IR (Russwurm and Childers, 2001; Hanst, 1971) Stephens and his group at the Environmental Protection Agency had already made measurements of ambient concentrations of peroxy acetyl nitrate (PAN) in the Los Angeles city basin before 1969 (Stephens, et al., 1969; Scott, et al., 1957). Aside from the apparently inconsequential controversy (since Hanst was part of the Stephen's group) valid questions on why is OP/FTIR is rarely used nowadays and why its development has been undermined with technological problems remain unanswered. Among possible answers to these questions stands out a limited sensitivity of the technique for atmospheric monitoring: 1-100 ppb by volume (contrasted to the requirements of parts per trillion by volume on many pollutants) and the lack of development of algorithms that can be incorporated into the instruments acquisition and analysis routines (software) that can make the use of the technique a more amenable and user friendly one. In a recent article by Griffiths and collaborators, the authors point out the difficulties encountered when using OP/FTIR that have led to a slow development of the remote sensing modality (Griffiths, et al., 2009). The clear advantages of wide area sensing and long range capabilities have been overshadowed by hardware and more so, by software limitations. Inadequacy in compensating for variable atmospheric contributions, mainly by water vapor and carbon dioxide has hampered the wide usage of OP/FTIR both in environmental studies as well as in Defense and Security applications. In this study, two types of FTIR standoff detection experiments were carried out: active mode OP/FTIR and passive mode OP/FTIR. The

detection of particle dispersion is also relevant to the forensic community. When an airbag deploys in an accident the lubricant is dispersed on the passenger. Many times the occupants in the vehicle are ejected or end up in a different location in the vehicle. Such a device could definitively place the occupants. Additionally, persons involved in the illicit manufacture of drugs will frequently retain chemical residues on their clothing. In this case, remote detection could be used to link a suspect to the crime scene.

There is a limited number of scientific contributions in the area of SOIR detection of HEM deposited on surfaces. Work by Theriault and colleagues (Theriault, et al., 2004), Van Neste and collaborators (Van Neste, et al., 2009), Blake and co-workers (Blake, et al., 2009) and Pacheco-Londoño and colleagues (Pacheco-Londoño, et al. 2009) have helped to contribute the development of this application of OP/FTIR. Theriault and collaborators made field measurements of liquid contaminants deposited on a number of surfaces at a standoff distance of 60 m using FTIR radiometry (Theriault, et al., 2004). Van Neste and collaborators described standoff detection measurements of trace quantities of surface adsorbed high explosives (Van Neste, et al., 2009). They used two quantum cascade lasers (QCL) operated simultaneously in the MIR, with tunable wavelength windows that match with absorption peaks of nitroexplosives tested. In this important contribution researchers demonstrated a sensitivity of 100 ng/cm<sup>2</sup> and a standoff detection distance of 20 m for surface adsorbed analytes such as explosives and chemical agent simulant tributyl phosphate. The detection of Explosives on metallic substrates is the first step in demonstrating the facility of passive and active open path FTIR detection for general use. Other substrates such as textiles, plastic, wood, and glass are less reflective and present a greater challenge. The emergence of alternative bright sources, such as QCL's, puts the active detection of explosive residues on real life materials over significant pathlengths within reach. Blake and colleagues recorded hyperspectral images of galvanized steel plates, containing cyclotrimethylenetrinitramine (RDX), using a commercial long-wave infrared imaging spectrometer at a standoff range between 14 and 50 m (Blake, et al., 2009). Pacheco-Londoño and collaborators built an active IR standoff detection system by coupling a bench FTIR interferometer to a gold mirror and external cryocooled detector assembly for detection of explosives present as traces on reflective surfaces (Pacheco-Londoño, et al. 2009). Source-target distances in the range of 1 – 3.7 m were studied and limits of detection (LOD) values obtained were 18 and 20 µg/cm<sup>2</sup> for TNT and RDX, respectively. The results of the prototype built were attributed to the use of a modulated MIR beam source that was able to cut down stray light from laboratory illumination.

## 2. Description of methodology

Open Path Infrared Spectroscopy is a well established technique for atmospheric sensing of gases and condensable vapors. In the current application, after validating the spectroscopic system in detection of gases and condensable vapors, a more challenging application was addressed: detection of solid samples deposited as trace contaminants on metallic surfaces were detected by OP/FTIR. Sample preparation is a critical task in the development of any analytical technique. Three steps were performed for standoff detection of explosives and other highly energetic materials deposited on Al plates:

- TNT samples were weighted and dissolved in dichloromethane.
- Mixtures were deposited on the Al plates using a Teflon stub and were then allowed to air-dry.

- OP/FTIR standoff detection experiments were carried out, both in active mode using a mid infrared (MIR) source and passive mode using a thermal excitation (utilizing a tungsten lamp).

These steps are illustrated in Fig. 1.

Background spectra of Al plates with no TNT deposited on them were run for every standoff distance tested in active mode. In the case of passive mode standoff detection, background spectra were acquired at every range value and every plate temperature tested. Then, statistical routines were applied using chemometrics. In particular, partial least squares (PLS) regression analysis was used to perform quantification studies of HEM surface loadings at all standoff distances. Standoff detection of solid samples present as traces on metallic substrates required a sample preparation methodology that would be able to deposit solid samples on a solid substrate, with high coverage uniformity and reproducibility. Due to the size of the substrates, sample smearing technique was used to deposit the HEM TNT at trace amounts on metallic substrates (Primera-Pedrozo, 2008). As shown in Fig. 2a, aluminum plates of areas  $30.5\text{ cm} \times 30.5\text{ cm}$  were used as material support for HEM samples. Dichloromethane was used to clean the aluminum surfaces. Plates were allowed to air-dry before of depositing the desired HEM surface loading. A small amount of dichloromethane was used to dissolve TNT sample to be deposited. A  $3\text{ cm} \times 15\text{ cm}$  Teflon stub was used to smear the HEM sample on the aluminum substrates (Fig. 2b). The amount of HEM that remained on the Teflon stub after sample smearing was negligible. The nominal surface concentrations obtained by the smearing technique were 50, 100, 200, 300, and  $400\text{ }\mu\text{g}/\text{cm}^2$  of HEM. Figs. 2b and 2c show how TNT was deposited on aluminum plates for 50 (Fig. 1b) and  $100\text{ }\mu\text{g}/\text{cm}^2$  (Fig. 1c), respectively.

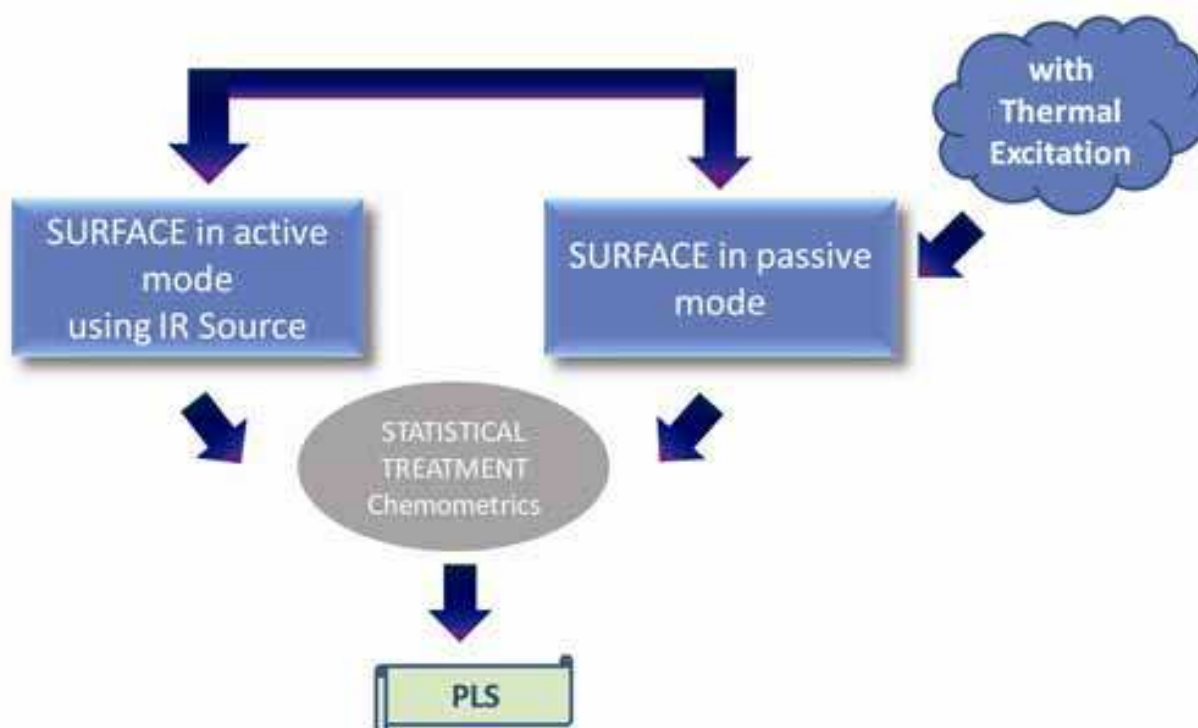


Fig. 1. Steps for remote detection of nitroexplosives and other HEM deposited on surfaces using OP/FTIR





Fig. 2. Sample preparation: (a) Clean Al plate ready for sample smearing technique; (b) 50 µg/cm² of TNT loading concentration; (c) 100 µg/cm² of TNT surface concentration

A model EM27 (Bruker Optics, Billerica, MA) OP/FTIR spectrometer, was used to obtain the MIR spectral information of TNT samples. Table 1 contains the specifications and technical data of the EM27. Fig. 3 illustrates the difference in operation between a benchtop FTIR spectrometer used in absorption mode (Fig. 3a) and an IR interferometer configured for open-path measurements (Fig. 3b). The optical bench consisted of a compact, enclosed, and desiccated Michelson type interferometer equipped with ZnSe windows, internal black body calibration source, KBr beamsplitter, f/0.9 and a field of view (FOV) of 30 mrad (1.7°). Its main features are: permanently aligned, vibration insensitive, and friction-free mechanical bearing. The system was capable of acquiring 32 spectra per second at 1 cm<sup>-1</sup> resolution.

PARAMETER	SPECIFICATION
<b>Spectral Range:</b>	700 – 1300 cm <sup>-1</sup> (useful for passive measurements) 700 – 4000 cm <sup>-1</sup> (useful for active measurements)
<b>Resolution:</b>	1.0 cm <sup>-1</sup> (Option: 0.5 cm <sup>-1</sup> )
<b>NEDT:</b> (Noise Equivalent Delta Temperature):	up to 0.08°C for one scan with a resolution of 1 cm <sup>-1</sup> and a mirror speed of 40 kHz, depending on the detector
<b>Optical Bench:</b>	compact, enclosed, desiccated, purge interferometer
<b>Beamsplitter:</b>	KBr-substrate with multi-layer coating (Option: ZnSe)
<b>Interferometer:</b>	vibration insensitive, friction-free mechanical bearing; permanently aligned; symmetrical interferogram acquisition at 4 scanning velocities up to 40 kHz
<b>Standard Detector:</b>	MCT-detector (narrow band), liquid nitrogen cooled,
<b>Field of View:</b>	30 mrad (10 mrad with receiver telescope)

Table 1. Specifications of EM27 Open Path FTIR spectrometer

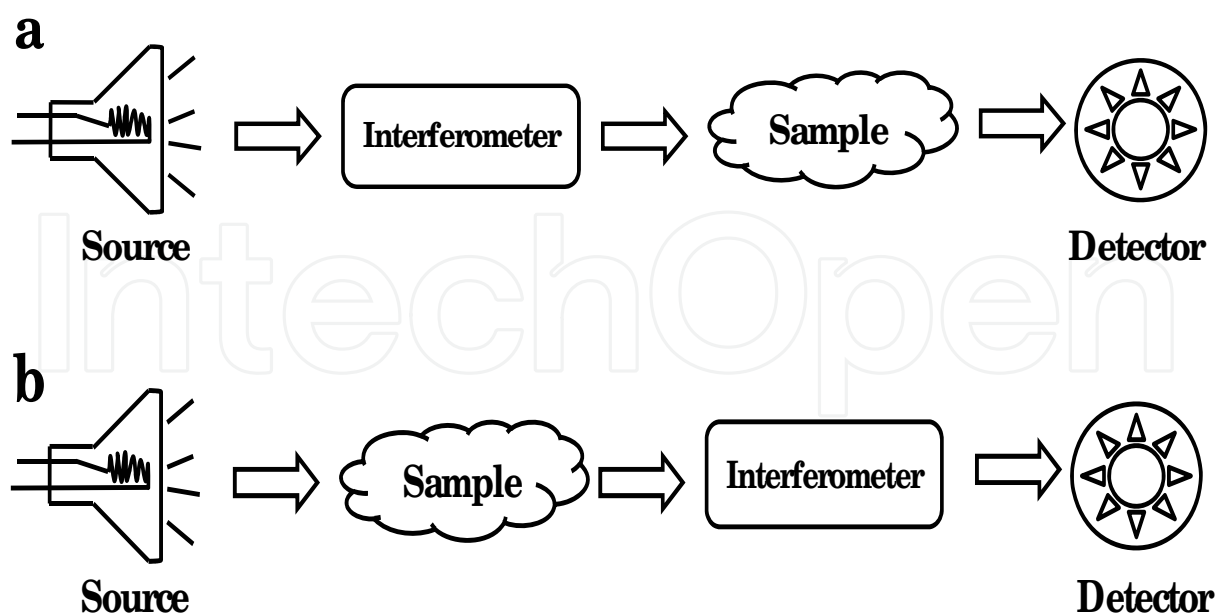


Fig. 3. FTIR interferometer configured as: (a) absorption spectrometer: detects source radiation only; (b) open-path spectrometer: detects source and sample radiation

High sensitivity measurements were achieved by using a high sensitivity closed cycle cryo-cooled photoconductive mercury cadmium telluride (MCT) MIR detector. Both, the MIR source and interferometer were focused on the target by MIR telescopes for active mode measurements (Fig. 3). Telescopic sights with mounts were used to align both source and collector. The transmitter source telescope was a 6 in. diam. F/4, gold coated mirrors with  $\text{FOV} \geq 7.5$  mrad; the receiver IR telescope was also a 6 in. diam. F/3 gold coated reflector with a FOV of 10 mrad. For passive mode measurements, the experimental setup was the same that in active mode, but the telescope coupled MIR source for excitation of the target was not used. Instead, a 500 W tungsten lamp was used to heat the aluminum plates with and without target analytes deposited on them. For both active mode and passive mode, multivariate calibrations were obtained and relevant statistical parameters were calculated and used as criteria to judge the quality of the method.

### 3. Application of multivariate calibrations to OP/FTIR data analysis

The mathematical modeling and detection of explosives and other threats in a complex environment can be complex. The large spectral bandwidth of a FTIR spectrometer facilitates the analysis. The purpose of calibration techniques is to correlate measured quantities such as the absorption of infrared radiation with properties of the system, for example, the concentration of one component in a multicomponent system. The accepted method of data analysis of gas phase contaminants present in a complex multicomponent mixtures as is the case of atmospheric pollutants present in air is classical least squares (CLS) regression analysis, also termed linear regression analysis or least squares (Russwurm and Childers, 1999). For quantification studies, CLS calibration curves can be generated using two methods: measurement of the absorbance peak heights and integration of areas in the spectral region of interest. Calibration plots using peak areas represents a better choice

for quantitative analysis when compared to peak height analysis (Lavine, 2002; Kramer, 1998). Usually, two steps are required: the calibration of the method and the analysis to determine a value of an unknown sample. It is important to emphasize that measuring surface concentrations using the peak area method is conceptually simple and easy to use, but it has some limitations. The method is univariate (the concentration is determined with a single spectral peak) and depends on a linear correlation between the concentration and the spectral response. The results can, therefore, be undermined by perturbations such as fluctuations caused by detector noise, temperature variations, or molecular interactions.

In a series of recent important papers by Griffiths and collaborators, the authors have demonstrated three important and novel aspects of data analysis for open path FTIR detection at a distance (Hart and Griffiths, 1998; Hart, et al., 200; Griffiths, et al. 2009; Shao, et al. 2010). Specific contributions can be summarized as follows:

- Establishment that multivariate data analysis techniques are required to exploit all the benefits that having a wealth of spectral information immersed in a congested multicomponent spectrum as that contained in SOIR experiments, not only for gas phase measurements but also for solid phase OP/FTIR detection at a distance, as Castro and collaborators have recently demonstrated (Castro, et al., 2010).
- Demonstration that a single background spectrum measured at a fixed source-target distance, temperature, pressure and ambient gases partial pressures can be used for all ranges and combinations of other relevant variables.
- Demonstration that the representation of OP/FTIR spectra in absorbance or percent transmission is equivalent. The output of any FTIR spectrometer is a single-beam spectrum that must be ratioed or compared (subtracted) against a appropriate background spectrum resulting in the transmittance spectrum of the sample,  $T(\nu)$ . In quantitative measurements, the transmittance should be converted to absorbance,  $A(\nu)$ , i.e.  $-\log_{10}\{T(\nu)\}$  since the absorbance is a linear function of the concentration of the species absorbing, thus rendering it more amenable to use of chemometrics routines of analysis. For the current application: OP/FTIR detection of solid threat chemicals deposited on surfaces as traces, representation as the spectral difference between the sample spectrum and the background spectrum is even more critical due to the possibility of specular reflectance and scattering from the sample (Castro, et al., 2010).

Multivariate calibrations make use of not only a single spectral point but take into account spectral features over a wide range. Therefore, the analysis of overlapping spectral bands or broad peaks becomes feasible. The information contained in the spectra of the calibration samples will be compared to the information of the concentration values using a PLS regression. The method assumes that systematic variations observed in the spectra are a consequence of the concentration change of the components. However, the correlation between the components concentration and the change in the infrared signal does not have to be a linear one.

Calibrations are typically constructed using chemometrics methods of data analysis such as the partial least squares (PLS) regression algorithm. The PLS algorithm is commonly incorporated in spectroscopic software such as OPUS™, Pirouette™ and Matlab Toolboxes™, among others. The advantages of using chemometrics for the quantification of organic compounds on glass, aluminum and stainless steel and other surfaces have



been discussed in the literature (Mehta, et al., 2003; Hamilton, et al., 2005; Perston, et al., 2007; Primera-Pedrozo, et al., 2004; Primera-Pedrozo, et al., 2005; Primera-Pedrozo, et al., 2007; Soto-Feliciano, et al., 2006; Primera-Pedrozo, et al., 2008; Primera-Pedrozo, O. M.; 2009).

PLS is a multivariate method that uses spectral features over a wide spectroscopic range. It is a spectral decomposition method that is intimately related to principal component analysis (PCA). In PCA, the spectral matrix is first decomposed into a set of eigenvectors and scores, and then a regression is performed against the concentrations as a separate step. However, PLS uses the concentration information during the decomposition process. In the case of OPUS™ (Bruker Optics), Quant2 software is used to find the best correlation function between the spectral information and the loading concentrations. Quant2 uses a partial least squares-1 (PLS-1) regression method. Calibrations are performed using PLS-1 in which only one component can be analyzed separately, instead of simultaneously analyzing multiple components, as in the PLS-2 routine of chemometrics. Then, cross validations are performed and the root mean square errors of the cross validations (RMSECV) and the root mean square errors of estimations (RMSEE) are used as criteria to evaluate the quality of the correlations obtained. In the standard “leave-out-one” cross validations, each spectrum is omitted from the training set and then tested against the model built with the remaining spectra. As illustrated in Tables 1 and 2, some explosives require spectroscopic preprocessing (except mean centering) and more PLS evaluations in order to obtain a good model. In the case of the first derivative, the Savitzky-Golay algorithm is actually used to obtain the derivative. The number of smoothing points used can be adjusted to suppress the effect of noise (Beebe, 1998). Other details of the advantages of using a chemometrics model such as PLS to correlate the loading concentration with IR spectra have been discussed in the literature (Hamilton, et al., 2005).

Multivariate calibrations require a large number of calibration samples and yield a large amount of data. In order to conveniently handle the data, the spectral information and the concentration information are written in the form of matrices, where each row in the spectral data matrix represents a sample spectrum. The concentration data matrix contains the corresponding concentration values of the samples. The matrices are then broken down into their eigenvectors which are called factors or principal components. Only the relevant principal components are used instead of the original spectral data, thus leading to a considerable reduction of the amount of data. A PLS regression algorithm will be developed to find the best correlation function between spectral and concentration data matrix (OPUS™, Bruker Optik, 2006). The OPUS/QUANT software package (OPUS™, Bruker Optik, 2006) is designed for quantitative analysis of spectra consisting of bands showing considerable overlap. The software allows determining the concentration of more than one component in each sample simultaneously. For this purpose, QUANT uses a **partial least squares (PLS)** regression method.

The residual (*Res*) is the difference between the true and the fitted value. Thus the **sum of squared errors (SSE)** is the quadratic summation of these values:

$$SSE = \sum [Res_i]^2 \quad (1)$$

The coefficient of determination (***R*<sup>2</sup>**) gives the percentage of variance present in the true component values, which is reproduced in the regression. ***R*<sup>2</sup>** approaches 100% as the fitted concentration values approach the true values:

$$R^2 = \left( 1 - \frac{SSE}{\sum (y_i - y_m)^2} \right) \times 100 \quad (2)$$

In the case of a cross validation, the **root mean square error of cross validation (RMSECV)** can be taken as a criterion to judge the quality of the method:

$$RMSECV = \sqrt{\frac{1}{M} \times \sum_{i=1}^M (y_i - y_{(i)})^2} \quad (3)$$

where  $M$  is the number of standards in the data set. One method of cross-validation is **leave-one-out cross-validation (LOOCV)**. Leave-one-out cross-validation is performed by estimating  $n$  calibration models, where each of the  $n$  calibration samples is left out one at a time in turn. The resulting calibration models are then used to estimate the sample left out, which acts as an independent validation sample and provides an independent prediction of each  $y_i$  value,  $y_{(i)}$ , where the notation  $i$  indicates that the  $i$ th sample was left out during model estimation. This process of leaving a sample out is repeated until all of the calibration samples have been left out. To obtain the **root mean square error of prediction (RMSEP)**, the validation samples prepared and measured independently from the calibration samples are used. The number of validation samples,  $p$ , should be large, so that the estimated prediction error accurately reflects all sources of variability in the calibration method. The **RMSEP** is computed as:

$$RMSEP = \sqrt{\frac{1}{p} \times \sum_{i=1}^p (y_i - y_{(i)})^2} \quad (4)$$

where  $p$  is the number of prediction samples.

Partial least squares (PLS) regression algorithm from Quant2 software of OPUS™ version 6.0 (Bruker Optics) was used to find the best correlation function between the spectral information and the surface concentration. PLS was used for generating a chemometrics model for all analyzed standoff distances. Cross validations were made and the root mean square errors of cross validations (RMSECV) and correlation coefficient ( $R^2$ ) were used as criteria to judge the quality of the correlations obtained at different standoff distances.

#### 4. OP/FTIR detection of gases and condensable vapors

Griffiths et al. described two general ways in which OP/FTIR can be used for remote sensing measurements (Griffiths, et al., 2009). When the source and the detector are in line of sight with each other and they have separate power sources the operational mode is called *bistatic*. In this setup, the source is non-modulated by the interferometer and as a result stray light contributions cannot be minimized. On the other hand, when all the components reside within the spectrometer, including the MIR source, sharing a common power source, the operational mode is termed *monostatic*. This setup has clear advantages as pointed out by Pacheco-Londoño and collaborators in reducing stray light components, but is limited to source power and cooling restraints (Pacheco-Londoño, et al., 2009). In the active mode employed for remote detection, a bistatic setup in which the source is not modulated was used.

The first task in evaluating the performance of the Bruker Optics EM27 open path interferometer was to use it in detection of gases and condensable vapors. The spectroscopic system was configured for *bistatic* operational mode in active configuration (Fig. 3b) with source and interferometer in line-of-sight of each other. Measurements were done for standoff distance of 1-10 m. The spectra of ambient air and ammonia ( $\text{NH}_3$ ) at 10 m range at room temperature are shown in Fig. 4a-d. In the case of  $\text{NH}_3$ , spectra were collected at an instrumental resolution of  $1\text{ cm}^{-1}$ . The presence of ro-vibrational lines in the remote IR absorption spectrum of ammonia is clearly shown in Figs. 4b and 4c. The intense spectrum obtained for dichloromethane is illustrated in Fig. 4d. Gas phase standoff IR spectra of some high vapor pressure liquids are shown in Fig. 5a-d. Spectra are arranged in increasing order of their room temperature vapor pressure and absorbance of most prominent spectroscopic features (vibrational signals). The presence of spectral contributions from ambient water vapor and carbon dioxide ro-vibrational lines can be seen. These persistent lines were not removed by any of the widely used algorithms since spectral windows for sample identification were available in all cases.

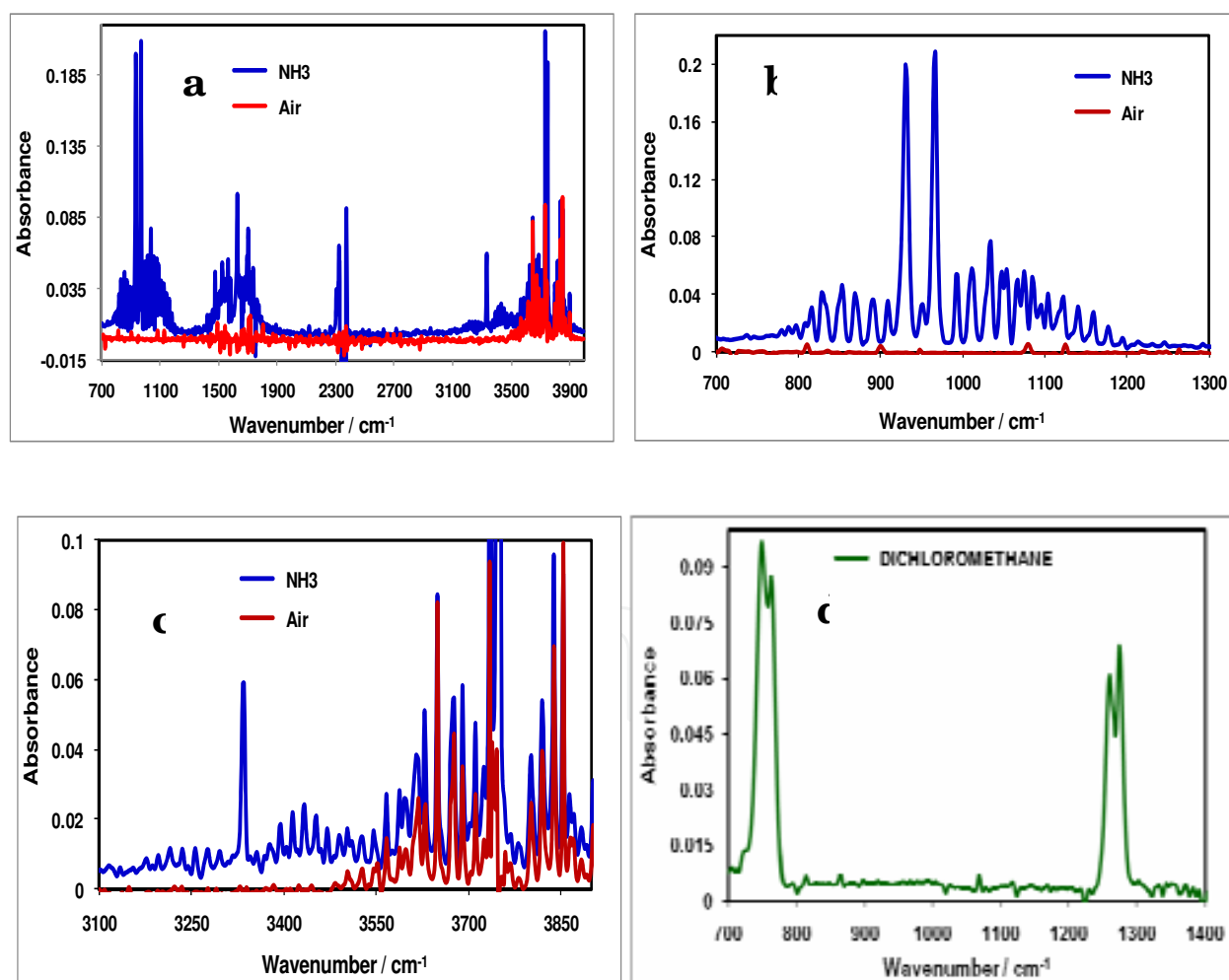


Fig. 4. Active mode OP/FTIR spectra of: (a) air and  $\text{NH}_3$  complete spectrum; (b), (c) details of  $\text{NH}_3$  spectrum; (d) dichloromethane

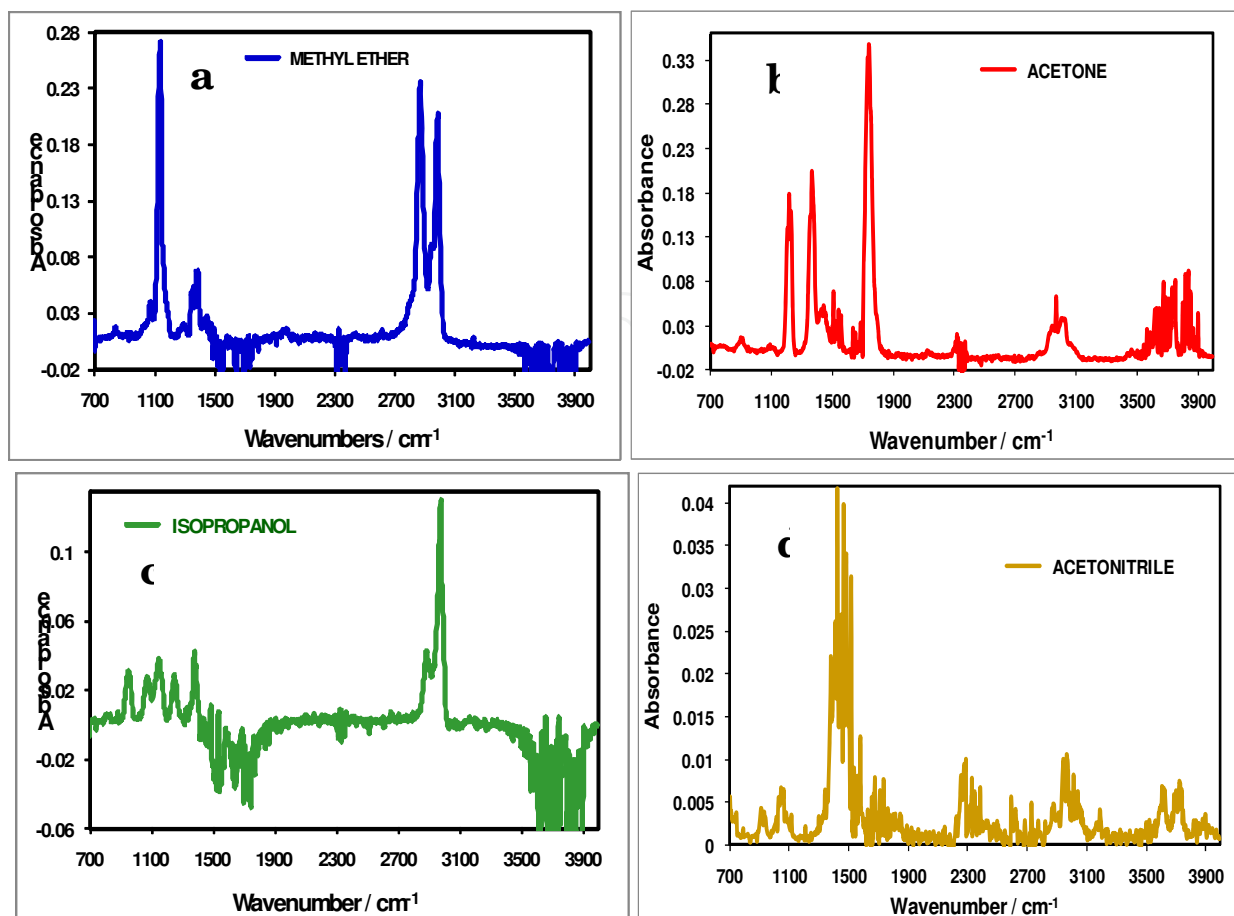


Fig. 5. Active mode remote spectra of condensable vapors: (a) methyl ether; (b) acetone, (c) isopropanol; acetonitrile

The spectral band shapes observed in stand-off detection mode, shown in Figures 4 and 5, are superimposed on a ramp-shaped background, and the bands themselves exhibit strong reflective (dispersive) band profiles. Since these measurements were done on a reflective metal substrate, the distortion of the band profiles is expected; similar effects have been reported in DRIFT (diffuse reflection infrared Fourier Transform) spectroscopy (Chalmers; Mackenzie, 1985), and in microscopically acquired infrared spectra of microspheres (Basan, et al. 2009a). In both cases, the distortion of the absorptive line shapes is due to the fact that within an absorption peak, the reflective index undergoes anomalous dispersion, as shown in Figure 6. In spectroscopic experiments carried out in reflectance mode, a mixing of the absorptive and dispersive line shapes can occur, resulting in bands that have a negative dip at the high wavenumber side of the peak, cf. Figures 4 and 5. This will shift the peak maximum by up to  $15\text{ cm}^{-1}$  toward lower values (Basan, et al. 2009b).

For 'real-life' stand-off detection, strong reflectance band distortions, such as those shown in Figures 4 and 5 are not likely, since these are typical for reflectance spectra on metals, and should be much weaker if explosives are distributed on fabric. However, mixing of absorptive and reflective line shapes can also be mediated by scattering effects (Basan, et al. 2009a) and could produce significant band distortions.

Unsupervised correction of the spectral distortions will be necessary since the distortions cause apparent frequency shifts which will confound spectral search and identification algorithms. Although several methods have been developed to correct the dispersive line

shapes observed in biological systems (Basan, et al. 2009a; Bird, et al. 2010) they are not applicable here, since they are based on multivariate methods, and require large number of spectra, as well as undistorted reference spectra. For the spectra reported here, a method originally published in 2005 (Romeo and Diem, 2005), may be more suitable. This method is based on phase correction between real and imaginary spectral contributions which can be obtained by reverse Fourier transform of the contaminated spectra. The original implementation of this method contained a minor logical error, which since has been corrected (Bird, et al. 2010).

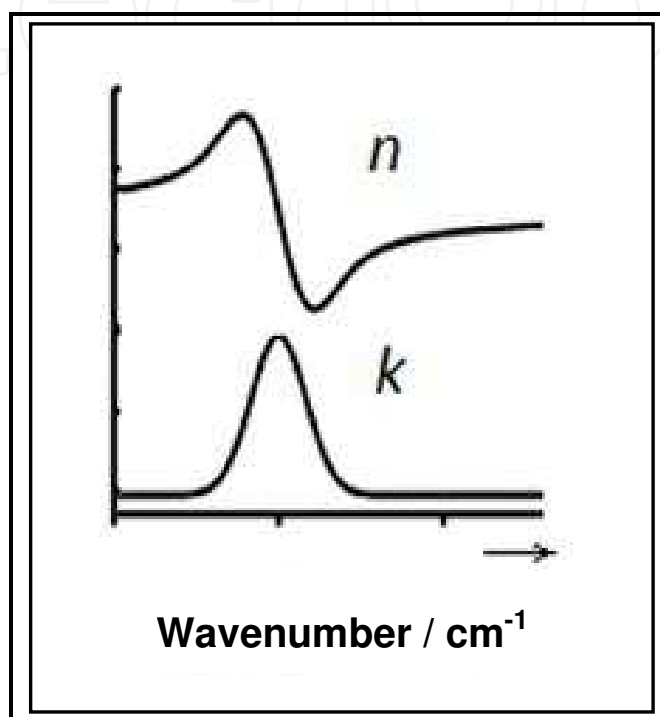


Fig. 6. Anomalous Dispersion of the refractive index ( $n$ ) in the vicinity of an absorption band

## 5. Active standoff IR detection of solids deposited on substrates

Active mode standoff IR measurements of solids, including nitroexplosives and other highly energetic materials (HEM) smeared on Al plates at various surface loadings were carried out. Spectra in the fingerprint region were obtained with EM27 spectrometer. In the active mode used in the current application, a bistatic operation setup in which an IR telescope was used to steer a MIR source which was not modulated and sat side by side to the reflective IR telescope collector, operating in back-reflection mode (Fig. 7). Initial experiments were done with solid samples deposited onto aluminum plates at the highest surface loading used:  $400 \mu\text{g}/\text{cm}^2$ . Samples were transferred to the metallic test substrates by dissolving in an appropriate solvent and then smearing them on the test plates. A Teflon stub was used to assist in sample smearing. Coated plates were allowed to dry in air at room temperature.

Initial remote IR experiments were designed to optimize experimental considerations, including sample placement and measurement geometry. For the reflectance IR measurements at one meter (1 m) standoff distance, as shown in Fig. 8, the angle of incidence of the MIR radiation (and angle of reflection) was varied from  $0^\circ$  to  $\sim 30^\circ$ . TNT signals decreased drastically at high incident angles, becoming nearly unobservable at  $27^\circ$ . Spectra of selected



solid phase compounds deposited as traces on Al substrates are shown in Fig. 9. A fixed standoff distance of 8 m and loading concentration of  $400 \mu\text{g}/\text{cm}^2$  was used for the SOIR measurements. The first spectrum of Fig. 9 is that of caffeine deposited on Al plate. Fig. 9b and 9c show the spectra of p-benzoic acid and benzoic acid, respectively at  $25^\circ\text{C}$ . For the acquisition of the data shown in Fig. 9d the sample plate was heated to  $28^\circ\text{C}$  to demonstrate how the emission of vibrational quanta is significantly enhanced by small temperature differences. The remote IR spectrum of aliphatic nitrate ester PETN is shown in Fig. 9e and the corresponding spectra aliphatic nitramine RDX are shown as %T and absorbance in Fig. 9f.

Pacheco and co-workers used a modulated home built setup for remote IR measurements of nitroexplosives from  $\sim 1 \text{ m}$  to  $\sim 4 \text{ m}$  range. At short distances (0.9 m and 1.8 m) the maximum and minimum signal to noise (SNR) values showed high dispersion. They found out that with their uncollimated MIR beam, the problem both was sample and transfer solvent dependent in the low to very low loading concentrations studied. They argued that part of the problem was the lack of uniformity in surface coverage due to nucleation and crystallization phenomena. When the IR beam used was 1-2 cm in diameter or less, sample discontinuities could be detected and this was reflected by the relatively high dispersion in the values of SNR. At longer target-collector distances (1.8, 2.7 and 3.7 m) the maximum and minimum SNR values were very close due to higher sample coverage by a beam spot of  $\sim 5 - 11 \text{ cm}$  in diameter. At a source-target distance of 0.9 m, limit of detection (LOD) value determined was  $2 \mu\text{g}/\text{cm}^2$  for TNT. According to the authors, LOD values determined could have been influenced by several factors, such as: humidity, alignment of detector, source pointing accuracy, detector efficiency and reflectivity of samples and substrates.

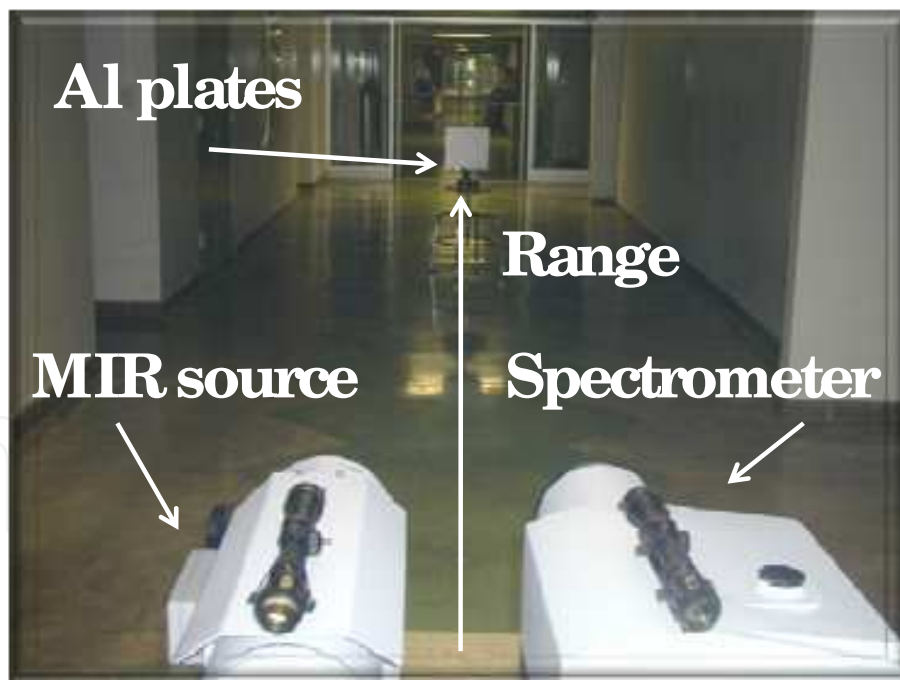


Fig. 7. Experimental setup used for SOIR detection. In active mode operation, both MIR source and FT interferometer were coupled to gold coated mirrors MIR reflective telescopes. In passive mode only the IR spectrometer was used

The reflectivity of sample: substrate and analyte, is mainly determined by how the analyte is deposited and by the solvent used for deposition. If the explosive exists on the surface as a thin layer, the backscattering signal is low but the reflection-absorption infrared (RAIRS)

spectra measured is of high signal-to-noise (SNR) value. When the explosive was present on the surface as discrete particles (crystals), the backscattered SIRS signal improved; correspondingly, the RAIRS signal measured for surface loading validation got worse. Sample smearing was done twice using the Teflon applicator: from left to right and then right to left. When the first pass was done the solvent was allowed to evaporate. Then, the second pass was carried out to induce more sample roughness and particle formation (crystallization) on the surface. TNT deposits on the substrate did not result in a thin layer covering the metallic surface. Instead droplets of a metastable phase were formed on the surface (Manrique-Bastidas, et al., 2004; Vrcelj, et al., 2001; Manrique-Bastidas, et al. (2) 2004). This metastable phase could be easily turned to its crystalline phase by friction, abrasion or even by pressing hard with the Teflon applicator for the sample smearing stage. This effect enhanced the SOIR experiments of TNT because the metastable phase was formed in the first smearing step. When the methanol evaporated and the second smearing stage was performed, crystalline roughness was induced resulting in a lower LOD value for TNT than for RDX. Standoff IR spectra of  $400 \mu\text{g}/\text{cm}^2$  TNT at 1 m and 14.5 m are shown in Fig. 10. A reference spectrum of neat, microcrystalline sample of TNT (1 mg/100 mg KBr) obtained in the macro sample chamber of a benchtop interferometer (Bruker Optics IFS-66/v) is included for comparison purposes.

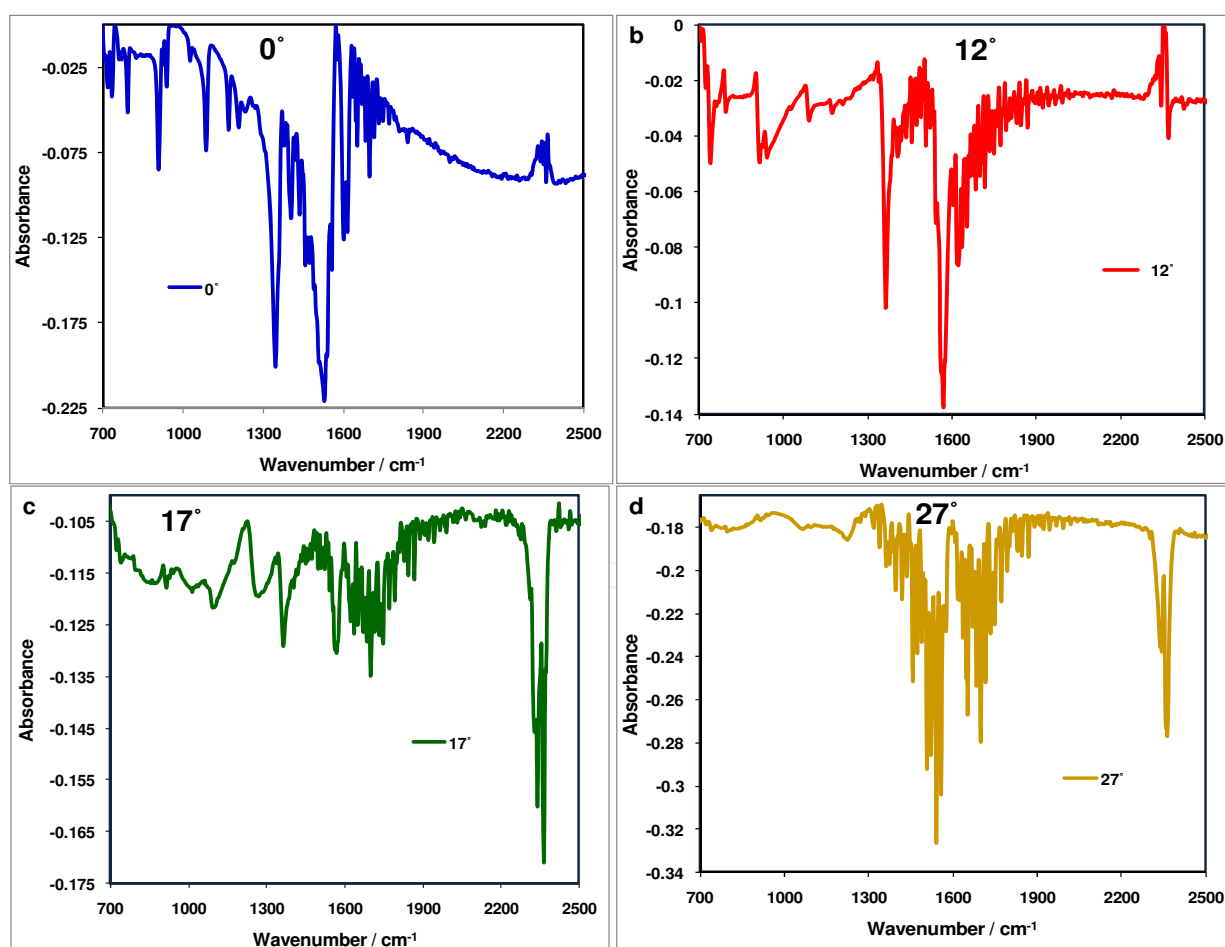


Fig. 8. Active mode OP/FTIR spectra of  $400 \mu\text{g}/\text{cm}^2$  TNT deposited on Al plate at: (a)  $0^\circ$ ; (b)  $12^\circ$ ; (c)  $17^\circ$ ; (d)  $27^\circ$ . Data shown demonstrates the specular reflectance nature of the IR reflection-absorption (transflection) experiment

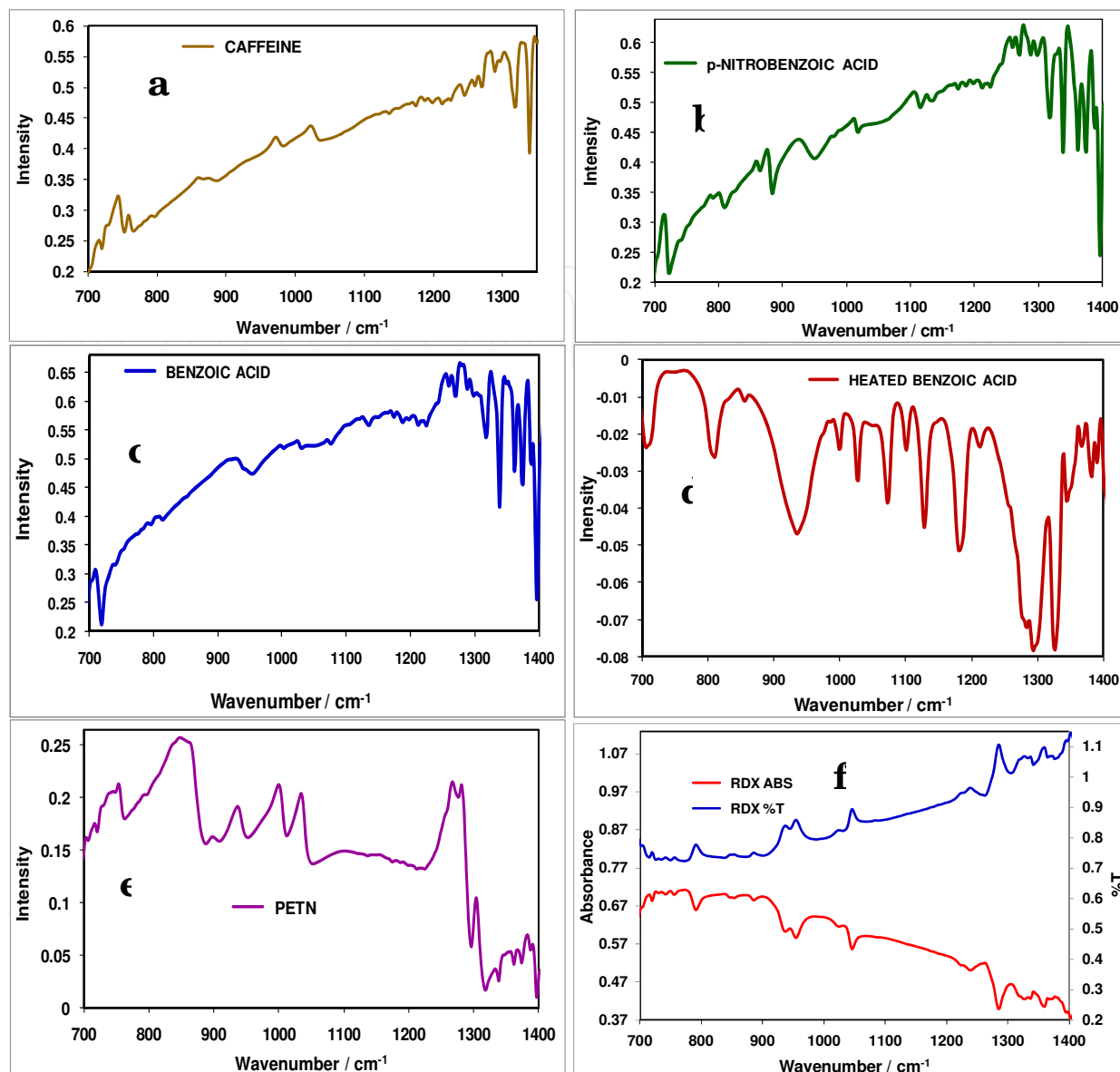


Fig. 9. Remote IR spectra of: (a) caffeine; (b) p-nitrobenzoic acid, (c) benzoic acid at room temperature (25 °C); (d) benzoic acid heated to 28 °C; (e) aliphatic nitrate ester PETN; (f) nitramine RDX in absorption and in %T

Other remote IR detection experiments were done using only TNT as target. Loading concentrations ranging from 50 to 400  $\mu\text{g}/\text{cm}^2$  of TNT were deposited on Al plates. The targets were carefully aligned to the source and collector and then the SOIR spectra were recorded. The analyzed target-collector distances were 4, 8, 12, 16, 20, 25, and 30 m. A total of 10 spectra were taken for each sample, at 20 scans and 4  $\text{cm}^{-1}$  resolution. Experiments were carried out at room temperature (25°C). Spectra were collected in remote, bistatic active mode detection IR at various surface concentrations at a fixed standoff distance of 8 m. Typical results are shown in Fig.11. These traces were not submitted to any pre-processing routine: offset correction, baseline correction, smoothing, water vapor rotational lines removal, etc. Thus, there is no common baseline for these spectra and some traces exhibit positive intensity ramps to higher wavenumber. However, increase of signal intensity as function of loading surface concentrations is clearly shown without the use of

chemometrics routines. Intense vibrational band about  $908\text{ cm}^{-1}$  was tentatively assigned to C-N stretching, vibrational band at  $938\text{ cm}^{-1}$  was assigned to C-H out-of plane bend (ring) and symmetric stretch band of the nitro groups appears at  $1350\text{ cm}^{-1}$ . Results agree with reported values (Pacheco-Londoño, et al., 2009; Clarkson, et al., 2003).

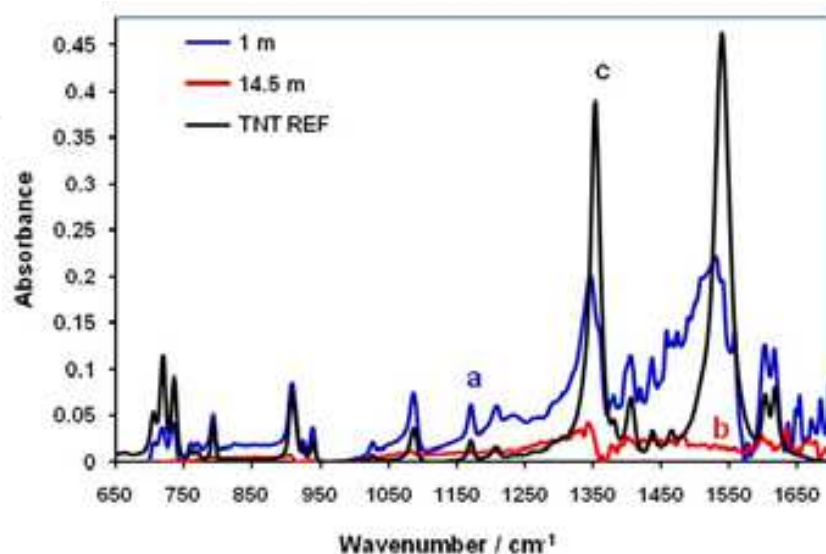


Fig. 10. Comparison of IR spectra of TNT: (a) KBr pellet with 1 mg TNT obtained in a macro sample compartment of a FTIR; (b) active mode SOIR spectrum of  $400\text{ }\mu\text{g}/\text{cm}^2$  deposited on Al plate measured at 1 m range distance; (c) same sample before measured at a source-target distance of 14.5 m. Prominent spectral features are present

When a MIR source was used for carrying out active mode experiments, the intensity of the peaks decreased when the distances increase. This is illustrated in Fig. 11a for spectra of Al plate coated with surface loading of  $400\text{ }\mu\text{g}/\text{cm}^2$  TNT and measured at standoff distances of 4, 8, 12, 16, 20, 25 and 30 m. At standoff distances higher than 25 m it was not possible to visualize clearly some of TNT vibrational signatures. At these distance the density of infrared radiation that gets to the Al plates from the MIR source is low, leading to a smaller number of excited molecules, so that the detector cannot register the low intensity signals emitted. Fig. 11b shows SOIR spectra of TNT as function of loading concentration. Spectra were collected in active mode detection standoff IR at a fixed standoff distance of 8 m.

The statistical treatments with chemometrics using PLS were carried out using the spectral region  $700\text{ to }1400\text{ cm}^{-1}$ , where the nitro symmetric stretch and aromatic C-H vibrations are present. Data pre-processing is an important stage in performing a calibration. Thus, the PLS models were built using mean centering as only pre-processing of variables. To ensure the reproducibility of the calibration samples, several spectra of each sample (fixed loading concentration and standoff distance) had to be acquired. If spectra of the same sample are not identical, a data pre-processing procedure must be chosen to bring them in line with each other. Data pre-processing can eliminate variations in offset or different linear baselines. Different treatments data were used, including: **vector normalization, first derivative and second derivative, mean-centering, but no other pre-processing routine was applied**, achieving best results for RMSECV and  $R^2$ . Results indicate that the experimental setup has good management of external variables, such as humidity, temperature changes, homogeneity of samples on Al plates, and others at ranges as far as 30 m and surface loadings of  $50\text{ }\mu\text{g}/\text{cm}^2$ .

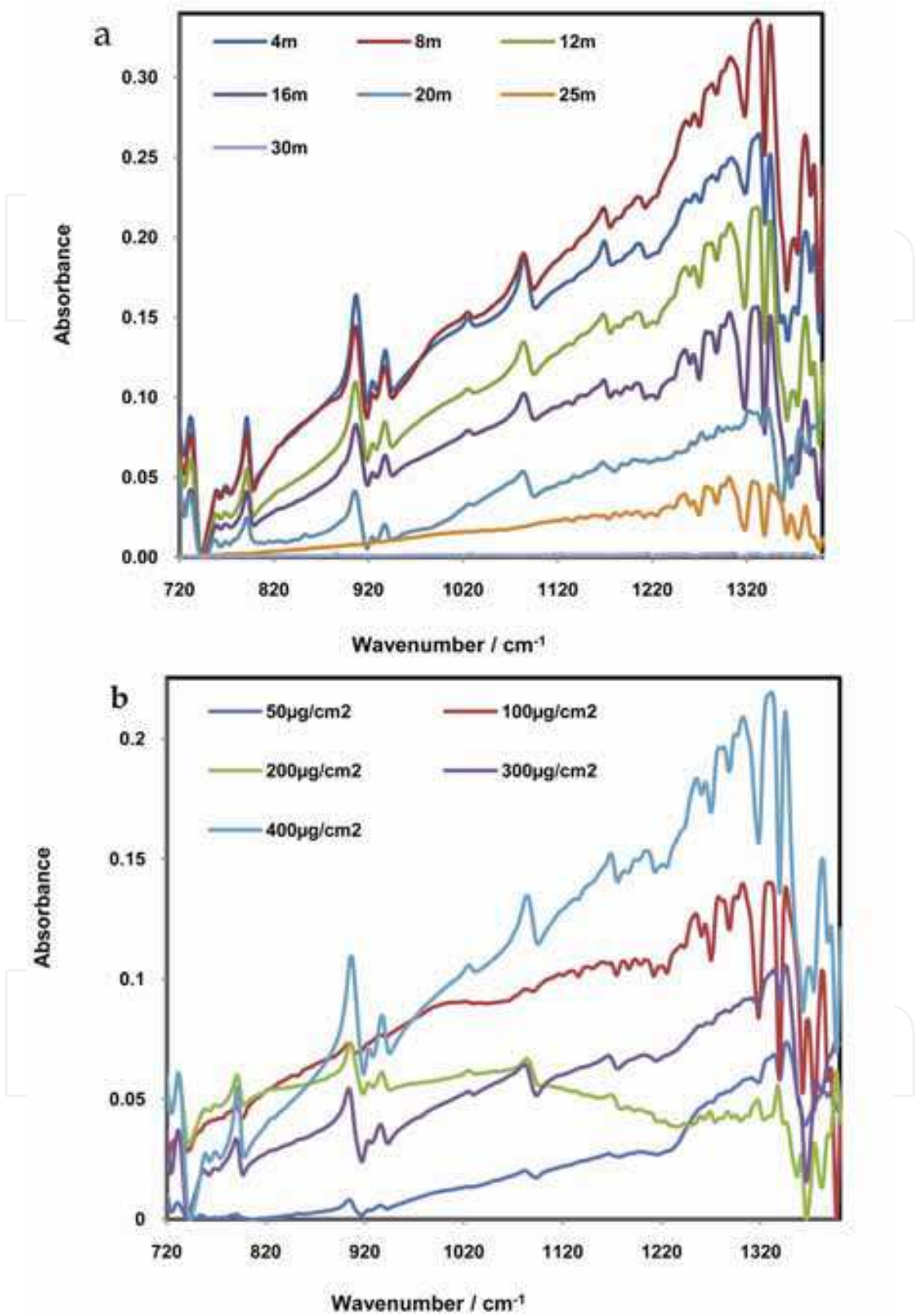


Fig. 11. Active mode FTIR spectra of TNT: (a) at different standoff distances of Al plate coated with surface concentration of 400 µg/cm<sup>2</sup>; (b) at several loading concentrations at fixed range of 8 m



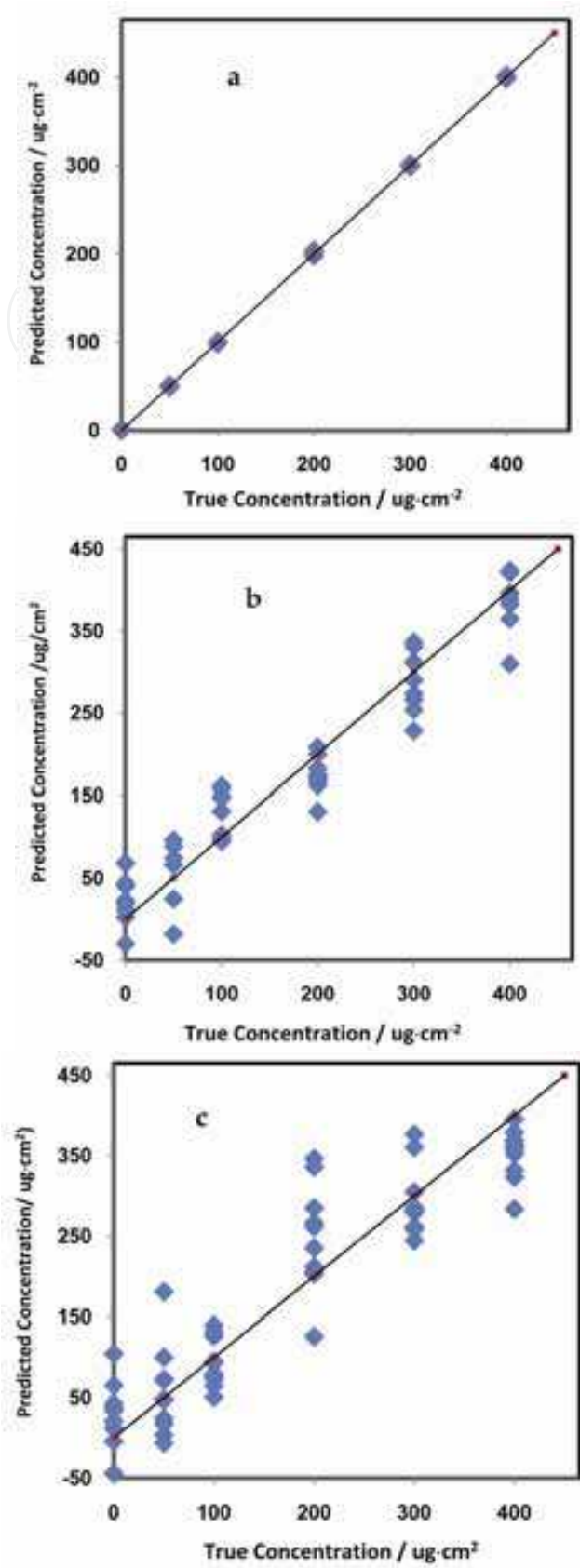


Fig. 12. Predicted loadings vs. true loadings for TNT on Al plates at various ranges using Opus 6.0™ Quant2: (a) 20 m; (b) 25 m; (c) 30 m

Fig. 12 illustrates the results obtained of the cross validation at the analyzed standoff distances: 20, 25 and 30 m and Table 2 summarizes the results of RMSECV and  $R^2$  obtained in the PLS models. In these correlation charts, each point represents ten spectra with a fixed surface concentration (0, 50, 100, 200, 300, or 400  $\mu\text{g}/\text{cm}^2$ ). All PLS correlation charts of predicted surface loading value vs. true surface concentration value for 4, 8, 12 and 16 m were similar to the correlation chart presented for 20 m standoff distance (Fig. 11a). As the standoff distance increases ( $> 20$  m) some of the spectral information is lost, causing the spectra for each sample to be slightly different from the others (within experimental error) thus making it difficult to predict its concentration (see Figs. 11b and 11c). Taking into account the low values of RMSECV and high values of  $R^2$  obtained at maximum distance of 20 m, the correlation (PLS) models are useful tools to determine precisely the surface concentration of TNT unknown samples using OP/FTIR spectroscopy. More precise alignment of both transmitter and receiver MIR telescopes would be required to perform similar correlations for ranges  $> 20$  m.

## 6. Passive mode standoff IR detection

The setup used for passive mode detection using thermal excitation of the sample is shown in Fig. 13. The MIR source and transmitter telescope were not used in these experiments. Temperature differences tested were 1 to 7°C in one degree interval. Aluminum plates (Fig. 13a) were heated by a 500 W tungsten lamp that was placed on back of the Al plates (Fig. 13b). The standoff distances studied were 8, 16 and 30 m. In passive mode experiments it is not so critical to carefully align the target and detector while recording the spectra. Ten spectra were taken for each sample, at 10 scans and 4  $\text{cm}^{-1}$  resolution for passive mode experiment.

The emission from a heated, uncoated with TNT Al plate, used as blank to measure background contributions is shown in Fig. 14. The corresponding blackbody spectrum of 400  $\mu\text{g}/\text{cm}^2$  TNT is also shown overlapping the blank Al plate spectrum. Both traces were measured at a range of 8 m and the plates were maintained at an equilibrium temperature of 32°C by heating with a 500 W tungsten lamp.

Fig. 15 shows the TNT IR vibrational signatures recorded with an EM27 spectrometer using passive mode standoff IR detection of Al plates heated with tungsten lamp to different surface temperatures from 25 to 32°C. These spectra were measured at a standoff distance of 16 m and a TNT surface concentration of 400  $\mu\text{g}/\text{cm}^2$ . Most of the characteristic vibrational signatures of TNT are well defined. The bands that allow identifying TNT were taken in the spectral region 700-1400  $\text{cm}^{-1}$ . Most of the persistent bands are observed and the standoff spectrum agrees very well with traditional infrared techniques: sample compartment, KBr pellet, micro-IR, attenuated total reflectance (ATR, both micro and macro) and grazing angle reflectance (GA, both micro and macro). Bands tentative assignments are: 910  $\text{cm}^{-1}$  (2,6- $\text{NO}_2$  scissors and C-N stretch); 1087  $\text{cm}^{-1}$  (C-H (ring) in-plane bend); 1171  $\text{cm}^{-1}$  (C-C in-plane ring trigonal bend, 2,4,6-C-N and C- $\text{CH}_3$  stretch) and 1350  $\text{cm}^{-1}$  due to the symmetric stretching vibration of the  $\text{NO}_2$  (nitro) group bond. TNT vibrational markers change significantly with surface temperatures. At 25°C (black spectrum, room temperature) TNT vibrational signatures are present, but they can barely be noticed at 16 m standoff distance. For the spectrum at 26°C (green spectrum) there is a significant increment in intensity of TNT vibrational signals.

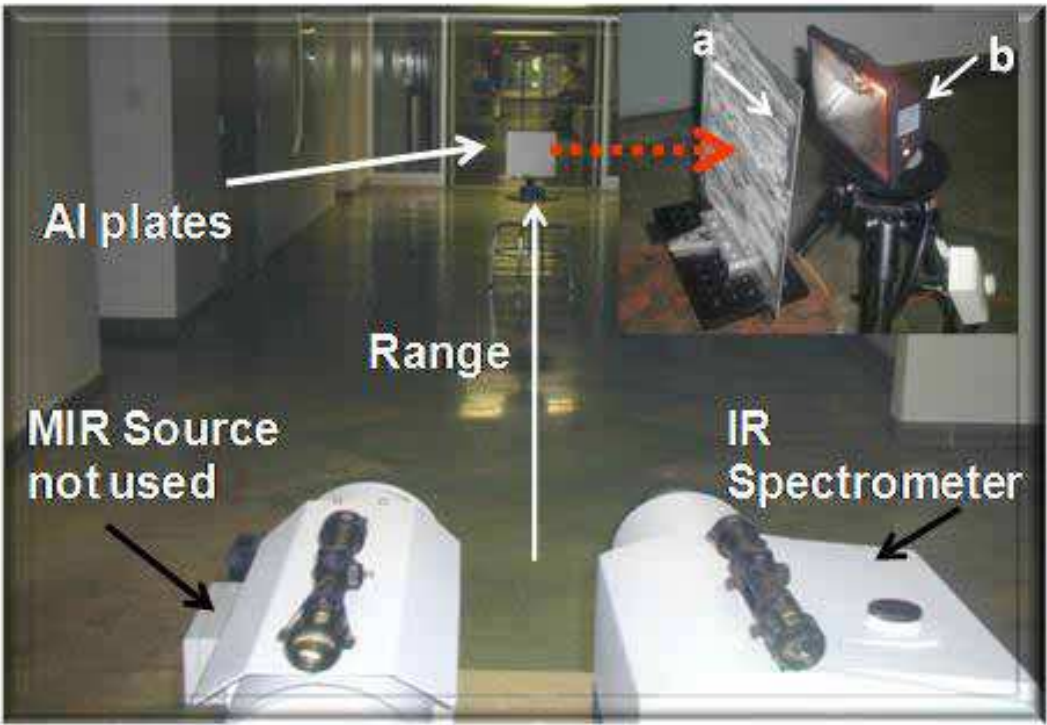


Fig. 13. Passive mode remote IR setup: (a) Al plate with TNT sample smeared-on; (b) 500 W tungsten lamp assembly

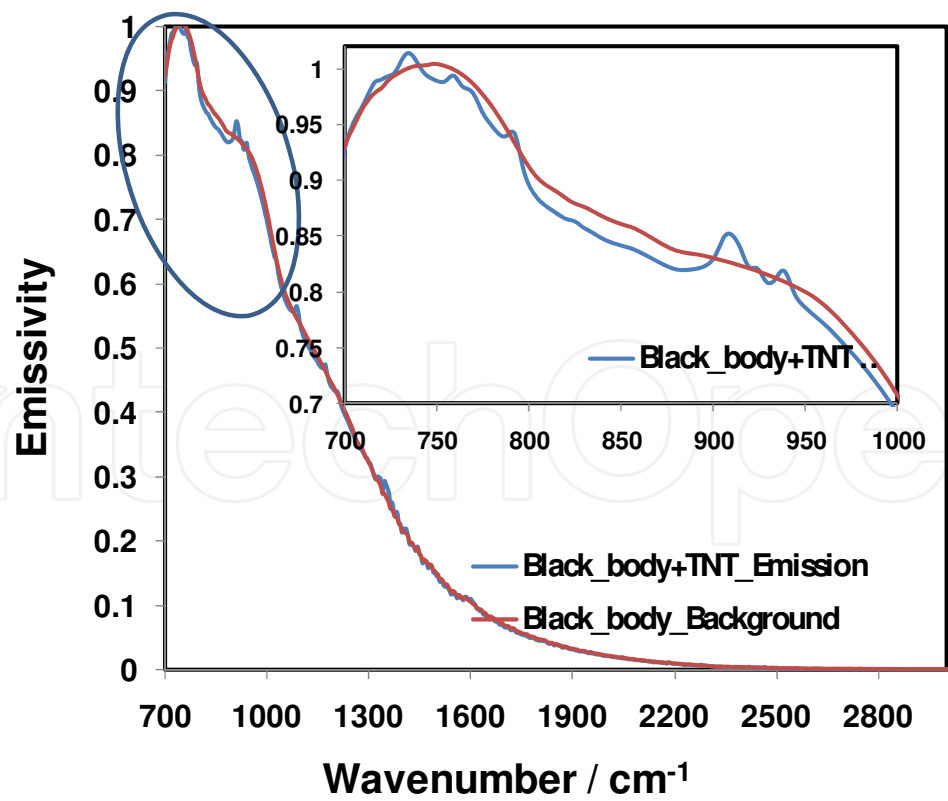


Fig. 14. Overlap of emissivity spectra of background air and air with TNT emissions from heated Al plate with 400  $\mu\text{g}/\text{cm}^2$  TNT at 8 m range and plate heated to 32°C

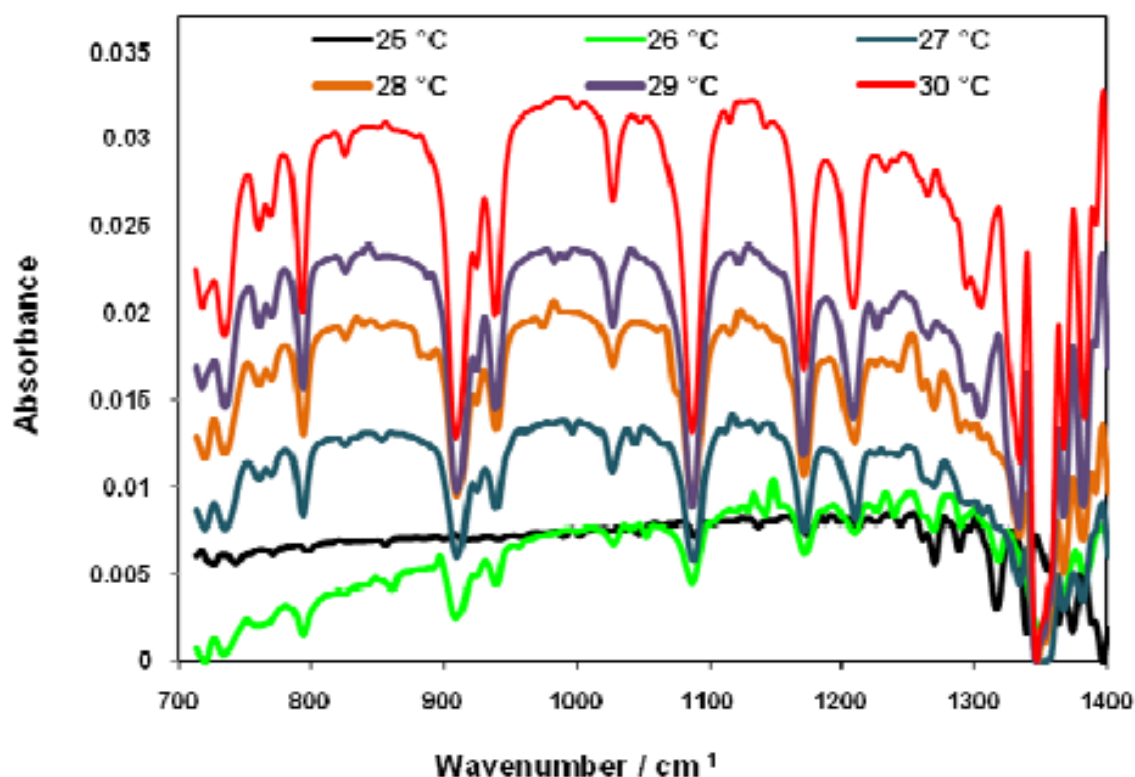


Fig. 15. Passive mode remote IR spectra of 400 $\mu\text{g}/\text{cm}^2$  TNT at several temperatures

The variation in peak areas with temperature for TNT for a surface loading of 200  $\mu\text{g}/\text{cm}^2$  at two different standoff distances is shown in Fig. 15. The vibrational spectra were measured out to a room temperature (25°C). For a standoff distance of 8 m (Fig. 11a) peak areas of the vibrational bands at 793 and 1087  $\text{cm}^{-1}$  were measured. For a standoff distance of 16 m the bands used for peak areas calculations were 793, 1087 and 1171  $\text{cm}^{-1}$  (Fig. 11b). In both cases when TNT was heated to higher temperatures more intense bands were observed. This study shows that the increase of the vibrational signatures has a second order polynomial behavior in all cases, with excellent correlation coefficients squared. These results are very useful for real field standoff detection, because when the target is warmer than room temperature, the vibrational signatures of the explosive are increased significantly.

The results of the effect of standoff distance on the intensity of heated samples are shown in Fig. 16. The spectra were taken at different distances and a specific surface temperature for each one. The tested temperature was always higher than the ambient temperature. Spectra taken at room temperature did not show some of the characteristic TNT vibrational signals (spectra not shown). Fig. 16 shows that the standoff detection in passive mode using thermal excitation is a useful tool for recording IR spectra to maximum range distance of 30 m, under the current experimental conditions.

PLS regression algorithm from Quant2 software for OPUS<sup>TM</sup>, version 6.0 (Bruker Optics, Billerica, MA) was used to find the best correlation function between the IR spectral information and the TNT surface concentration. PLS was used for generating a chemometrics model of analyzed standoff distances at specific temperatures (25 to 32°C). Cross validations were made and RMSECV and  $R^2$  were used as criteria to evaluate the quality of the correlations obtained. The statistical data treatments prepared using chemometrics routines (PLS) were carried out using spectral region 700 to 1400  $\text{cm}^{-1}$ , where

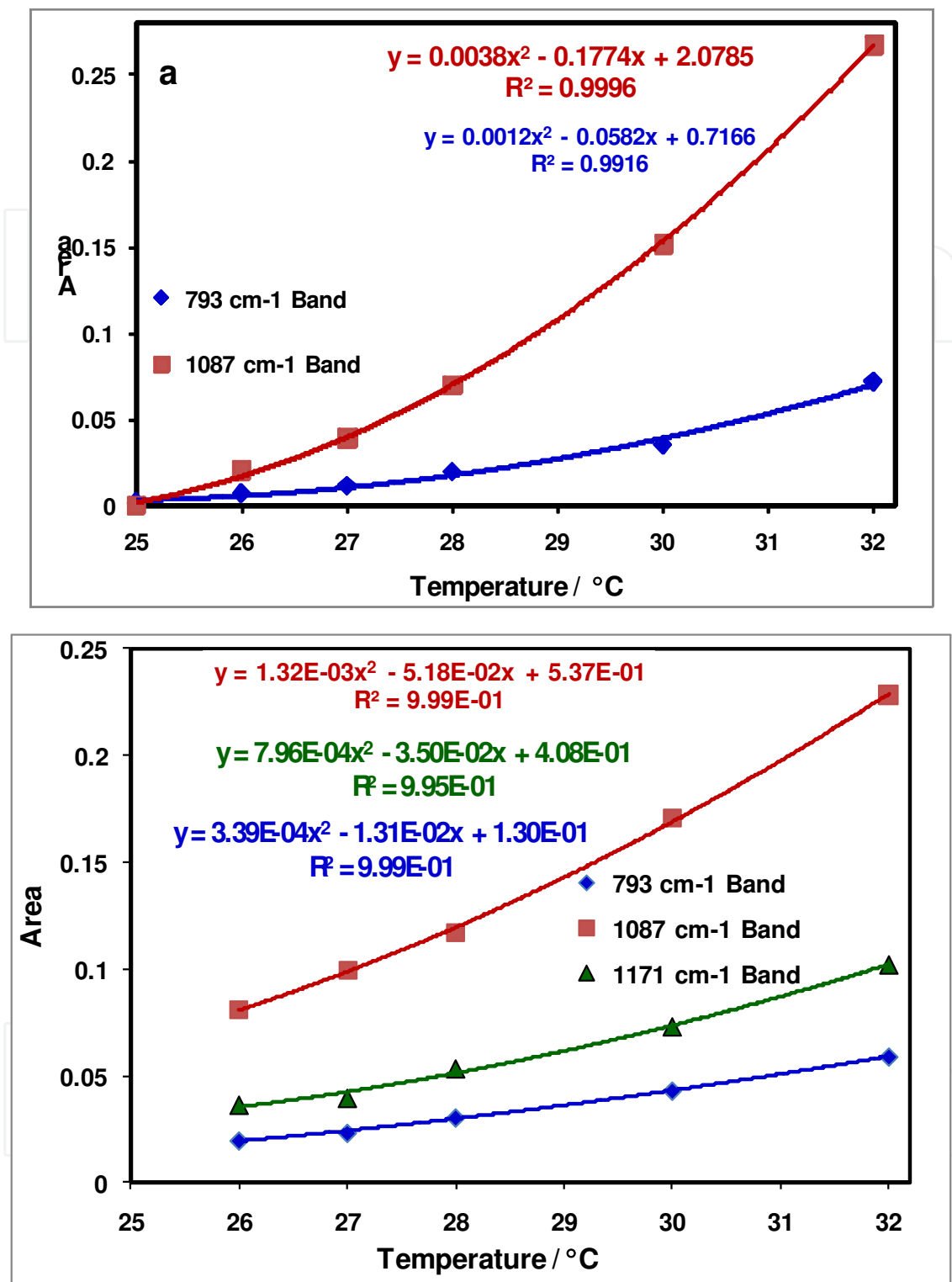


Fig. 16. Effect of temperature on intensity of TNT vibrational signals for 200 µg/cm<sup>2</sup> at range of: (a) 8 m; (b) 16 m

the nitro symmetric stretch and aromatic C-H and C-C vibrations are present. As before, PLS models were made using mean centering as pre-processing of variables. Data pre-processing included: “vector normalization, first derivative and second derivative but NO pre-processing” achieving best results for RMSECV and R<sup>2</sup>. Fig. 14 shows the results obtained



for the cross validations at analyzed standoff distances using different surface temperatures. Table 3 contains the summary of results for RMSECV and R<sup>2</sup> obtained in the PLS models.

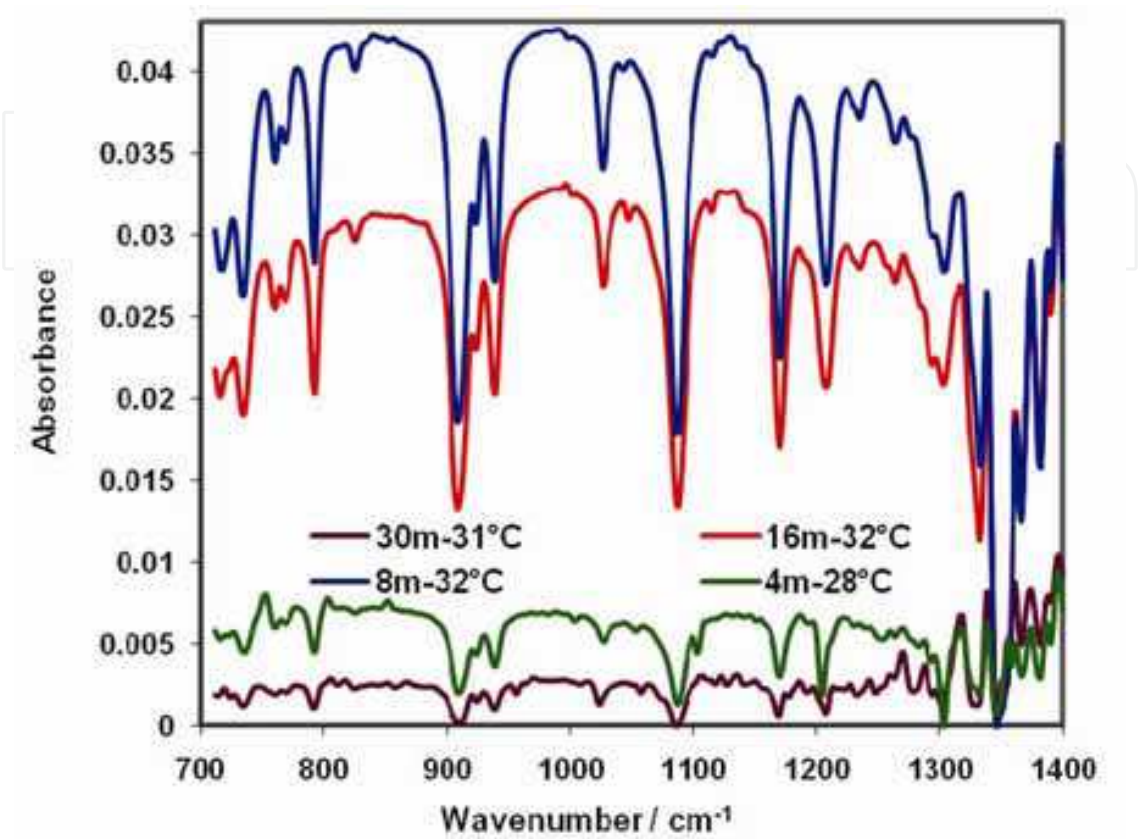


Fig. 17. Effect of the standoff distance on intensity of TNT IR signals. Surface concentration of 400  $\mu\text{g}/\text{cm}^2$  and 8-16 m range at sample temperatures: 28-32°C

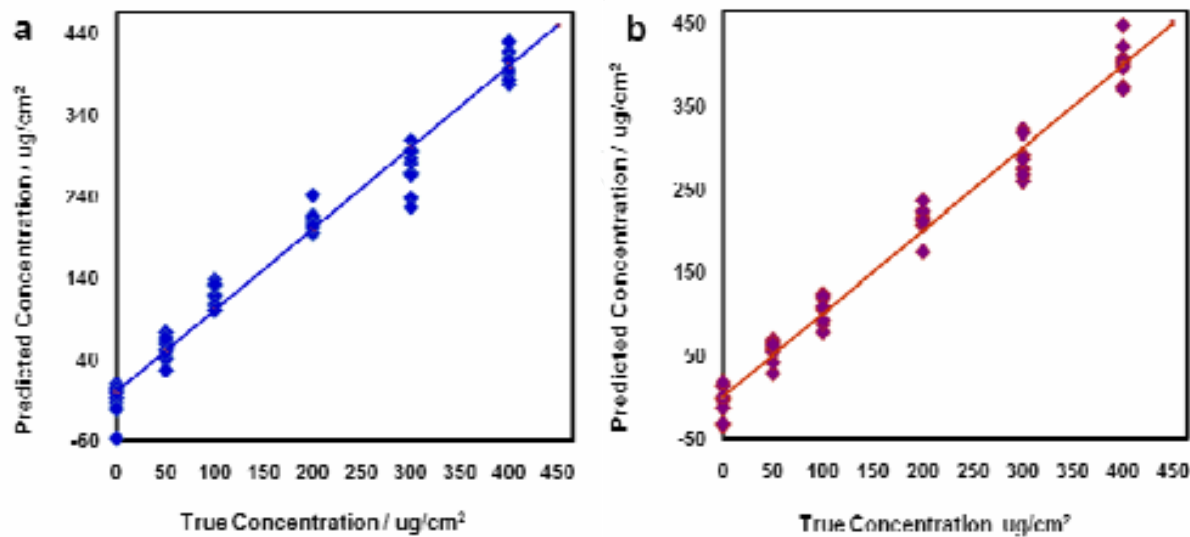


Fig. 18. Predicted vs. true surface concentration for TNT explosives at different standoff distances and temperature in passive mode: (a) 8 m range, 32 °C surface temperature; (b) 16 m range, 32 °C surface temperature

Standoff Distance (m)	Temperature (°C)	R <sup>2</sup>	RMSECV	RMSEP	Rank
8	25	0.9461	32.6	28.1	6
8	26	0.9737	22.8	29.2	9
8	27	0.9864	16.4	22.8	3
8	28	0.9692	24.7	24.3	2
8	30	0.9658	26.0	28.1	4
8	32	0.9760	21.8	17.7	6
16	25	0.9555	29.7	24.0	3
16	26	0.9624	27.3	29.0	3
16	27	0.9202	39.7	41.4	3
16	28	0.9567	29.3	27.6	4
16	30	0.9506	31.3	30.5	3
16	32	0.9684	25.0	26.6	3

Table 3. PLS calibration parameters for the different tested standoff distances and temperatures. Spectral range: 700 – 1400 cm<sup>-1</sup>; no preprocessing

All graphs of predicted vs. true surface concentration for specific distance and temperature (Table 3) have similar behavior to that of Fig. 18a for standoff distance of 8 m and Fig. 18b at a range of 16 m. Each point represents ten spectra with a specific surface concentration (0-400 µg/cm<sup>2</sup>). Taking into account the high values of R<sup>2</sup> (~ 0.96) and relatively low values of RMSECV (around 26.0) obtained for all the tested distances and temperatures these models could be used as a tools to determine the surface concentration of unknown samples of TNT at remote distances using SOIR.

7. Conclusion

A standoff technique using an Open-Path Fourier transform infrared (OP/FTIR) spectrometer has been demonstrated to obtain spectral information of TNT samples deposited on Al plates. The system consisted in an infrared telescope coupled MIR source and an IR coupled EM27 spectrometer manufactured by Bruker Optics. The remote

detection IR system was first tested for the standoff detection of gases and condensable vapors, which is the application that was developed for. High quality measurements were achieved by using a sensitive photoconductive cryo-cooled MCT detector. Standoff detection both in active and passive modes proved to be useful for recording TNT vibrational signatures in the range from 700 to 1400  $\text{cm}^{-1}$  of the MIR. Very good results of RMSECV and  $R^2$  were obtained in cross validations for active and passive mode experiments. The active mode standoff detection worked very well for distances lower than 30 m. Is necessary carefully aligning the target with the detector to be able to measure with high accuracy at ranges higher than 30 m.

For passive mode experiments thermal excitation proved to be a useful tool for enhancing TNT vibrational signatures for standoff detection. Achieving temperature difference of just 1°C between the sample and the spectrometer was enough to bring out spectral information to standoff distances of 8, 16 and 30 m. The increase in intensity of TNT signatures as a function of temperature can be modeled very well with second order polynomials in the temperature range tested above room temperature. In this experiment alignment of sample and detector was not critical as in the standoff active modality configuration. Partial least squares routines of commercial chemometrics statistical routines of spectroscopic analysis were used to enhance the data in multivariate mode.

## 8. Acknowledgments

Parts of the work presented in this contribution were supported by the U.S. Department of Defense, University Research Initiative Multidisciplinary University Research Initiative (URI)-MURI Program, under grant number **DAAD19-02-1-0257**. The authors also acknowledge contributions from Mr. Aaron LaPointe from Night Vision and Electronic Sensors Directorate, Fort Belvoir, VA, Department of Defense, Dr. Jennifer Becker MURI Program Manager, Army Research Office, DoD and Dr. Stephen J. Lee Chief Scientist, Science and Technology, Office of the Director, Army Research Office/Army Research Laboratory, DoD.

Support from the U.S. Department of Homeland Security under Award Number **2008-ST-061-ED0001** is also acknowledged. However, the views and conclusions contained in this document are those of the authors and should not be interpreted as necessarily representing the official policies, either expressed or implied, of the U.S. Department of Homeland Security.

## 9. References

- ALERT Department of Homeland Security university based Center of Excellence: at Northeastern University: <http://www.northeastern.edu/alert/index.php/>
- ALERT Department of Homeland Security university based Center of Excellence: at University of Rhode Island: <http://energetics.chm.uri.edu/>
- Akhavan, J. (2004). *The Chemistry of Explosives*. 2<sup>nd</sup> ed. T J International Ltd, Padstow, Cornwall, UK.
- American Society for Testing and Materials (1997) *Standard guide for open-path Fourier-transform infrared (OP/FTIR) monitoring of gases and vapors in air*, E-1865-97. In:

- Annual book of ASTM standards*, American Society for Testing and Materials, West Conshohocken, PA, vol 03.06.
- Bacci, M.; Fabbri, M.; Picollo, M.; Porcinai, S. (2001). Non invasive fibre optic Fourier Transform-infrared reflectance spectroscopy on painted layers identification of materials by means of principal component analysis and Mahalanobis distance. *Anal. Chim. Acta* 446, 15-21.
- Bangalore, A.S.; Small, G.W.; Combs, R.J.; Knapp, R.B.; Kroutil, R.T.; Traynor, C.A.; Ko, J.D. (1997) *Anal. Chem.* 69, 2, 118.
- Blake, T.A.; Kelly, J.F.; Gallagher, N.B.; Gassman, P.L.; Johnson, T.J. (2009) *Anal. Bioanal. Chem.* 395, 337.
- Beebe, K.; Pell, R.; Beth, M. (1998) *Chemometrics: A Practical Guide*. John Wiley & Sons. N.Y
- Caron, T.; Guillemot, M.; Montméat, P.; Veignal, F.; Perraut, F.; Prené P.; Serein-Spirau, F. (2010) *Talanta* 81, 1,543.
- Castro-Suarez, J.R.; Pacheco-Londoño, L.C.; Vélez, M.; Diem, M.; Tague, Jr. T.J.; Hernandez-Rivera, S.P. (2010) submitted, *Appl. Spectrosc.*
- Clarkson, J.; Smith, W.E.; Batchelder, D.N.; Smith, D.A. Coats, A.M. (2003) *J Molec. Structure*, 648, 203.
- Committee on the Review of Existing and Potential Standoff Explosives Detection Techniques, Existing and Potential Standoff Explosives Detection Techniques (2004) National Academies Press: Washington, DC.
- Diem, M. (1993). *Introduction to Modern Vibrational Spectroscopy*, John Wiley, New York, NY.
- Griffiths, P. R.; de Haseth, J. A. (2007) *Fourier transform infrared spectrometry*, 2nd ed. Wiley Interscience, Hoboken, NJ, pp 466-479.
- Griffiths, P.R.; Shao, L.; Leytem, A.B. (2009) *Anal. Bioanal. Chem.* 393, 45.
- Gunzler, H.; Gremlich, H.-U. (2002) *IR Spectroscopy: An Introduction*. Wiley-VCH, DE.
- Hamilton, M. L.; Perston, B. B.; Harland, P. W.; Williamson, B. E.; Thomson, M. A.; Melling, P. J. *Organic Process Research & Development*. 2005, 9, 337-343.
- Hart, B.K., Griffiths, P.R. (1998) Proc 11th Int. Conf Fourier Transform Spectrosc. *Am. Inst. Phys. Conf. Proc.* 430:241-242.
- Hart, B. K.; Berry, R. J.; Griffiths, P. R. (2000) *Environ. Sci. Technol.* 34:1346-1351.
- Hilmi, A.; Luong, J. (2000) *Environ. Sci. Technol.*, 34, 14, 3046.
- Huberty, C.J. (1994) *Applied Discriminant Analysis*. Wiley-Interscience, Hoboken, NJ.
- Johnson, R.A.; Wichern, D.W. (1992) *Applied Multivariate Statistical Analysis*. Prentice-Hall: Englewood Cliffs, NJ.
- Kramer, R., (1998). *Chemometrics Techniques for Quantitative Analysis*, Marcel Dekker, New York, NY.
- Lin-Vien, D.; Colthup, N.B.; Fateley, W.G.; Grasselli, J.G. (1991) *The Handbook of Infrared and Raman Characteristic Frequencies of Organic Molecules*. San Diego, CA pp. 179-189.
- Manrique-Bastidas, C.A.; Castillo-Chará, J.; Mina, N.; Castro, M.E.; Hernández-Rivera, S.P. (2004a), *Proc. SPIE Int. Soc. Opt. Eng.* Eng. 5415: 1345.
- Manrique-Bastidas CA, Primera-Pedrozo OM, Pacheco-Londoño LC, Hernández-Rivera, S.P. (2004b) *Proc. SPIE Int. Soc. Opt. Eng.* 5617: 429.
- Mardia, K.V.; Kent, J.T.; Bibbly, J.M. (1979) *Multivariate Analysis*. Academic Press: New York, N.Y.

- Marshall, M.; Oxley, J.C. (2009) *Aspects of Explosives Detection*. Elsevier, Amsterdam, The Netherlands.
- Mehta, N. K.; Goenaga-Polo, J. E.; Hernández-Rivera, S. P.; Hernández, D.; Thomson, M. A.; Melling, P. J. *Spectroscopy*, April, 2003.
- Miller, C. J.; Yoder, T.S. (2010) *Sens. Imaging: An International Journal*. 11, 2, 77.
- OPUS version 4.2 (2003) *User Manual*. Bruker Optics: Billerica, MA.
- OPUS version 6.0 (2006) *Spectroscopic software manual* Bruker Optik GmbH, DE.
- Pacheco-Londoño, L.C.; Ortiz, W.; Primera, O.M.; Hernández-Rivera, S.P. (2009) *Anal. Bioanal. Chem.* 395, 323.
- Parmeter, J. E. (2004) Proceedings of the 38th Annual 2004 International Carnahan Conference on Security Technology; 355 IEEE: New York.
- Perston, B.B.; Hamilton, M.L.; Williamson, B.E.; Harland, P.W.; Thomson, M.A.; Melling, P.J. (2007) *Anal. Chem.*, 79, 1231–1236.
- Primera-Pedrozo, O.M.; Pacheco Londono, L.C.; De la Torre-Quintana, L.F.; Hernandez-Rivera, S.P.; Chamberlain, R.T.; Lareau, R.T. (2004) *Proc. SPIE Int. Soc. Opt. Eng.* 5403, 237–245.
- Primera-Pedrozo, O.M.; Pacheco-Londono, L.C.; Ruiz, O.; Ramírez, M.; Soto-Feliciano, Y.M.; De La Torre-Quintana, L.F.; Hernandez-Rivera, S.P. (2005) *Proc. SPIE Int. Soc. Opt. Eng.* 5778, 543–552.
- Primera-Pedrozo, O. M.; Rodríguez, N.; Pacheco-Londoño, L. C.; Hernández-Rivera, S. P. (2007) *Proc. SPIE Int. Soc. Opt. Eng.*, 6542, 65423J.
- Primera-Pedrozo, O.M.; Soto-Feliciano, Y.; Pacheco-Londoño, L.C.; Hernandez-Rivera, S.P. (2008) *Sens. Imaging: An International Journal*. 9, 27–40.
- Primera-Pedrozo, O.M.; Soto-Feliciano, Y.; Pacheco-Londoño, L.C.; Hernandez-Rivera, S.P. (2009) *Sens. Imaging: An International Journal*. 10, 1–13.
- Soto-Feliciano, Y.; Primera-Pedrozo, O.M.; Pacheco-Londoño, L. C.; Hernandez-Rivera, S.P. (2006) *Proc. SPIE Int. Soc. Opt. Eng.* 6201, 62012H.
- Russwurm, G. M.; Childers, J.W (1999) *FTIR open-path monitoring guidance document*, 3rd ed., TR-4423-99-03. ManTech Environmental Technology. Research Triangle Park, NC, USA.
- Russwurm, G.M.; Childers, J.W. (2001) *Open-path Fourier transform infrared spectroscopy*. In: Chalmers, J.W.; Griffiths, P. R. (eds.) *Handbook of vibrational spectroscopy*, vol. 2. Wiley, Chichester, UK.
- Yinon, J.; Zitrin, S. (1996) *Modern Methods and applications in analysis of explosives*. John Wiley & Sons Ltd., Chichester, UK.
- Sharma, S.P.; Lahiri, S.C. (2008) *Spectrochim. Acta Part A*, 70, 144.
- Shao, L.; Griffiths, P.R.; Leytem, A.B. (2010) *Anal. Chem.* 82, 8027–8033.
- Smith, B. (2000) *Fundamentals of Fourier Transform Infrared Spectroscopy*. CRC Press, Boca Raton, FL, USA.
- Szkal, C.; Brewer, T.M. (2009) *Anal. Chem.*, 81, 13, 5257.
- Theriault, J.M.; Puckrin, E.; Hancock, J.; Lecavalier, P.; Lepage, C.J.; Jensen, J.O. (2004) *Appl Opt*, 43, 5870.
- Urbanski, T. (1964). *Chemistry and Technology of Explosives*. Vol. 1, Macmillan Co.: New York, NY.
- Van Neste, C.W.; Senesac, L.R.; Thundat, T. (2009) *Anal. Chem.* 81, 5, 1952.



Yinon, J. (1996) *J Chrom. A*, 742, 1, 205.

Vrcelj, R.M.; Gallagher, H.G.; Sherwood, J.N. (2001) *J Am. Chem. Soc.* 123:2291.

Weber, K.; Fischer, C.; van Haren, G.; Krause, H.; Bunte, G.; Schweikert, W.; Härdle, T. (2006) *Stand-Off Detection of Explosives of Suicide Bombers by Means of Open-Path FTIR Spectroscopy* in Schubert, H.; Rimski-Korsakov, A. *Stand-Off Detection of Suicide-Bombers and Mobile Subjects*, Proceedings of the NATO Advanced Research Workshop on Stand-Off Detection of Suicide Bombers and Mobile Subjects, NATO Security through Science Series B: Physics and Biophysics, Pfinztal, Germany, Springer, DE.



## **Fourier Transforms - New Analytical Approaches and FTIR Strategies**

Edited by Prof. Goran Nikolic

ISBN 978-953-307-232-6

Hard cover, 520 pages

**Publisher** InTech

**Published online** 01, April, 2011

**Published in print edition** April, 2011

New analytical strategies and techniques are necessary to meet requirements of modern technologies and new materials. In this sense, this book provides a thorough review of current analytical approaches, industrial practices, and strategies in Fourier transform application.

### **How to reference**

In order to correctly reference this scholarly work, feel free to copy and paste the following:

John R. Castro-Suarez, Leonardo C. Pacheco-Londoño, Miguel Vélez-Reyes, Max Diem and Thomas J. Tague, Jr. and Samuel P. Hernandez-Rivera (2011). Open-Path FTIR Detection of Explosives on Metallic Surfaces, Fourier Transforms - New Analytical Approaches and FTIR Strategies, Prof. Goran Nikolic (Ed.), ISBN: 978-953-307-232-6, InTech, Available from: <http://www.intechopen.com/books/fourier-transforms-new-analytical-approaches-and-ftir-strategies/open-path-ftir-detection-of-explosives-on-metallic-surfaces>

**INTech**  
open science | open minds

### **InTech Europe**

University Campus STeP Ri  
Slavka Krautzeka 83/A  
51000 Rijeka, Croatia  
Phone: +385 (51) 770 447  
Fax: +385 (51) 686 166  
[www.intechopen.com](http://www.intechopen.com)

### **InTech China**

Unit 405, Office Block, Hotel Equatorial Shanghai  
No.65, Yan An Road (West), Shanghai, 200040, China  
中国上海市延安西路65号上海国际贵都大饭店办公楼405单元  
Phone: +86-21-62489820  
Fax: +86-21-62489821

© 2011 The Author(s). Licensee IntechOpen. This chapter is distributed under the terms of the [Creative Commons Attribution-NonCommercial-ShareAlike-3.0 License](https://creativecommons.org/licenses/by-nc-sa/3.0/), which permits use, distribution and reproduction for non-commercial purposes, provided the original is properly cited and derivative works building on this content are distributed under the same license.

IntechOpen

IntechOpen